LATE PROTEROZOIC TRANSITIONS IN CLIMATE, OXYGEN, AND TECTONICS, AND THE RISE OF COMPLEX LIFE

NOAH J. PLANAVSKY[1], LIDYA G. TARHAN[1], ERIC J. BELLEFROID[1], DAVID A. D. EVANS[1], CHRISTOPHER T. REINHARD[2], GORDON D. LOVE[3], AND TIMOTHY W. LYONS[3]

[1]Department of Geology and Geophysics, Yale University, New Haven, CT 06520, USA <noah.planavsky@yale.edu>

[2]School of Earth and Atmospheric Sciences, Georgia Institute of Technology, Atlanta, GA 30332, USA

[3]Department of Earth Sciences, University of California-Riverside, Riverside, CA 92521, USA

ABSTRACT.—The transition to the diverse and complex biosphere of the Ediacaran and early Paleozoic is the culmination of a complex history of tectonic, climate, and geochemical development. Although much of this rise occurred in the middle and late intervals of the Neoproterozoic Era (1000–541 million years ago [Ma]), the foundation for many of these developments was laid much earlier, during the latest Mesoproterozic Stenian Period (1200–1000 Ma) and early Neoproterozoic Tonian Period (1000–720 Ma). Concurrent with the development of complex ecosystems, changes in continental configuration and composition, and plate tectonic interaction have been proposed as major shapers of both climate and biogeochemical cycling, but there is little support in the geologic record for overriding tectonic controls. Biogeochemical evidence, however, suggests that an expansion of marine oxygen concentrations may have stabilized nutrient cycles and created more stable environmental conditions under which complex, eukaryotic life could gain a foothold and flourish. The interaction of tectonic, biogeochemical, and climate processes, as described in this paper, resulted in the establishment of habitable environments that fostered the Ediacaran and early Phanerozoic radiations of animal life and the emergence of complex, modern-style ecosystems.

INTRODUCTION

The late Proterozoic was witness to perhaps the most profound biological and geochemical transition in Earth's history. In contrast, the preceding billion years appear to be characterized by biogeochemical, climatic, and evolutionary stasis. For example, there is little to no evidence for continental ice sheets of any kind during this time interval (flippantly termed the "boring billion"), suggesting climatic stability, and unusually invariant carbon isotope data attest to the stability of the global carbon cycle. The late Proterozoic, in contrast, was characterized by extreme biogeochemical and climatic volatility, as recorded by pronounced and rapid variability in the carbon isotope record and the stratigraphic record of repeated low-latitude glaciations of unparalleled scale and severity (Canfield, 2005; Lyons et al., 2012; Knoll, 2014). Moreover, the late Proterozoic records the evolution and diversification of eukaryotes, the earliest evidence for metazoan life, and dramatic reorganization of surface-ocean and benthic ecosystems and environments. As such, this period likely provides an early glimpse of the regulatory feedbacks that, in the modern ocean, control the interactions among organisms and biogeochemical cycling in Earth's surface environments. Recent work also suggests that this interval corresponded to a shift in the marine redox landscape, as well as surface-ocean oxygen levels (Lyons et al., 2014; Thomson et al., 2014). Conventionally, Neoproterozoic oxygenation is considered to be a unidirectional process, but it is likely that the Neoproterozoic, and potentially even the early Paleozoic, were characterized by dynamic swings in oxygen levels.

The emerging view is that there are three concurrent, but likely not coincidental, phenomena characterizing the early Neoproterozoic Earth system: 1) a shift in ecosystem structure and function within the

In: *Earth-Life Transitions: Paleobiology in the Context of Earth System Evolution. The Paleontological Society Papers, Volume 21, P. David Polly, Jason J. Head, and David L. Fox (eds.). The Paleontological Society Short Course, October 31, 2015.*

ocean, including the rise of eukaryotic algal primary producers and the eventual emergence of metazoan life; 2) severe low-latitude glaciation (the so-called 'Snowball Earth' events) and carbon cycle instability; and 3) further and potentially dramatic oxygenation of Earth's surface. The goal of this paper is to review the timing and mechanistic relationships among these phenomena and to discuss our view of the development and interaction of these factors may have shaped Earth's environments and biosphere. We also hope to elucidate the role—if any—that tectonic forcing may have played in controlling the observed Neoproterozoic biogeochemical transitions. An unusual concentration of continental area in the tropics is generally accepted to have been a key factor in the development of extensive, 'Snowball'-scale glaciation. For example, a preponderance of continental landmass at low latitudes would have allowed for continued chemical weathering of the continents, and thus extended carbon dioxide drawdown, as the ice sheets advanced toward lower latitudes. However, it is unclear if this configuration was unique to the early Neoproterozoic relative to the preceding billion years, and thus may have been only one of several controlling factors. Finally, shifts in the flux of volcanogenic carbon dioxide or variations in the composition of the upper continental crust may have also been key contributing factors to the climatic shifts recorded in the stratigraphic record (Godderis et al., 2003; McKenzie et al., 2014), and further exploration of these ideas is essential in order to reconstruct the mechanisms that regulated the biological, chemical, and physical dynamics of the Neoproterozoic world.

This paper reviews current records of late Paleoproterozoic to early Neoproterozoic (1.8 Ga to 0.7 Ga) paleobiological diversity and paleoecological complexity, marine redox regimes, paleoclimate, atmospheric oxygen levels, paleogeography, and crustal composition. We then explore relationships between these records and several Earth-system models that link climate, tectonics, and geochemical cycling to the initial radiation of eukaryotes and complex ecosystems.

THE RISE OF EUKARYOTES: THE PROTEROZOIC FOSSIL RECORD

The composition, complexity, and distribution of modern marine ecosystems are engineered dramatically by the presence of eukaryotes and the operation of eukaryote-driven processes. Eukaryotic behavior, ranging from phytoplanktonic carbon fixation to filter-feeding, carnivory, bioturbation, and reef-building at diverse scales and trophic levels, influences habitability and colonization. These relationships also shape sedimentological processes and regulate biogeochemical cycling. In so doing, eukaryotes mold the physical, chemical, and biotic landscape of both the benthos and the surface ocean. As such, their appearance and radiation, which shifted the world's oceans from a prokaryotic to eukaryotic mode, likely had a concomitantly substantial impact upon environments as well as biogeochemical and biotic processes (Fig. 1). Reconstructing the timing and nature of this transition, however, has been limited by the ability to constrain the first appearance of the earliest eukaryotes and to track their subsequent diversification—a task complicated by the likelihood that early eukaryotic life was small, single-celled, and soft-bodied. Efforts to reconstruct the early eukaryote record have been hampered by issues of both preservation and recognition (Knoll, 2014). However, recent efforts at improved sample collection, fossil detection and imaging, assessments of syngeity, and reconstruction of micro- and macro-scale taphonomic processes (e.g., Javaux et al., 2004; Grey and Calver, 2007; Anderson et al., 2014) are beginning to fill the gaps in the fossil record. The encouraging result is a clearer picture of early Earth ecosystems at the dawn of eukaryotic life.

Historically, molecular-clock estimates for the origin of eukaryotes range widely from the Archean to the Paleoproterozoic, Mesoproterozoic, or even the Neoproterozoic (e.g., Cavalier-Smith, 2002; Douzery et al., 2004; Hedges et al., 2004; Yoon et al., 2004). The molecular (biomarker) record of fossil lipids can, in certain cases, fingerprint eukaryotes or even particular eukaryotic clades. However, Archean and Proterozoic biomarker data are susceptible to artifacts due to issues of high maturity and contamination, and these factors need to be assessed carefully. Rigorous self-consistency checks are needed to verify syngeneity of any organic compounds detected; thus, biomarker evidence for eukaryotes other than from the youngest intervals of the Proterozoic has largely been equivocal (e.g., Blumenberg et al., 2012; Pawlowska et al., 2013; French et al., 2015).

Efforts to differentiate early, single-celled

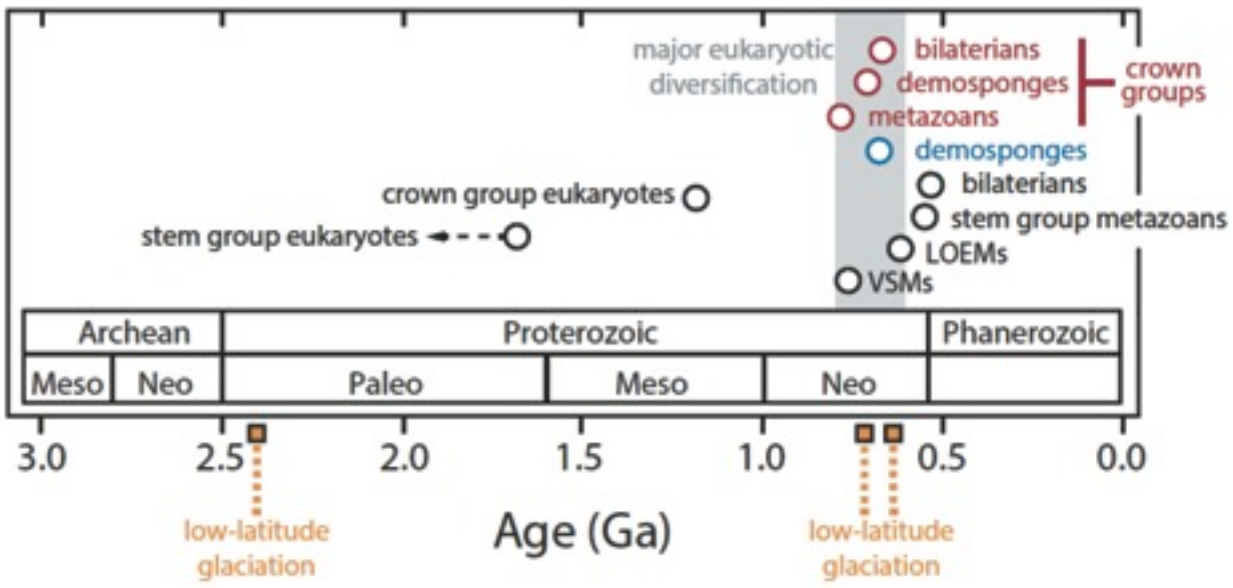

FIGURE *1*.—Approximate dates for the first appearance of various eukaryotic groups in the body fossil record (open black circles), the molecular fossil record (open blue circle), and best estimates from molecular clock techniques for the emergence of major crown groups (open red circles). Also shown are the fossils appearances of large ornamented Ediacaran microfossils (LOEMs) and vase shaped microfossils (VSMs). The vertical gray field denotes an interval of major eukaryotic diversification. After Planavsky et al. (2014).

eukaryotes from prokaryotes in the body-fossil record have also not proven to be straightforward, nor without controversy. Eukaryotes tend to be larger than prokaryotes and to possess complex morphology (e.g., ornamentation) and wall ultrastructure. However, these characters are also each known to occur in various prokaryotic groups (e.g., Schulz et al., 1999). Nonetheless, although not diagnostic when viewed individually, the combination of these characters is unknown in prokaryotes, so a microfossil characterized by all three of these traits can be most parsimoniously interpreted as eukaryotic in affinity (Knoll et al., 2006; Javaux, 2007; Knoll, 2014).

Challenges in detecting the last common ancestor (LCA) of eukaryotes extend to the differentiation of syngenetic and biogenic features from those attributable to diagenetic and abiogenic processes or contamination. Further confounding these studies are issues of morphological convergence and the differentiation of stem- from crown-group taxa (Javaux et al., 2010; Knoll, 2014). Efforts at actualistic morphological and ecological comparison are also hampered by limited understanding of modern protistan groups and even their recent evolutionary history (c.f., Knoll, 2014). Given these uncertainties, hypotheses for the evolutionary origin and phylogenetic placement of eukaryotes are wide-ranging, including an archaeal origin, based on common ancestry (Woese et al. 1990; Spang et al., 2015), or an archaeal 'host' (Williams et al., 2012, 2013), as well as eukaryogenesis through archaeal-bacterial symbiosis (Martin and Müller, 1998; Moreira and Lopez Garcia, 1998). Based on a combination of fossil and molecular evidence, the eukaryotic LCA likely appeared in the Mesoproterozoic and was a protist characterized by mitochondrial aerobic respiration and a mobile and heterotrophic life mode with various life stages (Javaux, 2007; Knoll, 2014).

The oldest potentially eukaryotic body fossils occur in the latest Paleoproterozoic Changzhougou Formation (ca. 1.8 Ga) and Chuanlinggou Formation (ca. 1.7 Ga) of North China (Lamb et al., 2009; Peng et al., 2009). These acritarchs (organic-walled microfossils), although of simple leiospheric morphology, range up to 250 μm in diameter, contain medial splits that may record encystment, and may also be characterized by complex wall structure (Lamb et al., 2009; Peng et al., 2009). However, identification of these fossils as eukaryotic is ambigious, and a stem-group affinity cannot be ruled out. The oldest microfossils to which a eukaryotic affinity can confidently be assigned

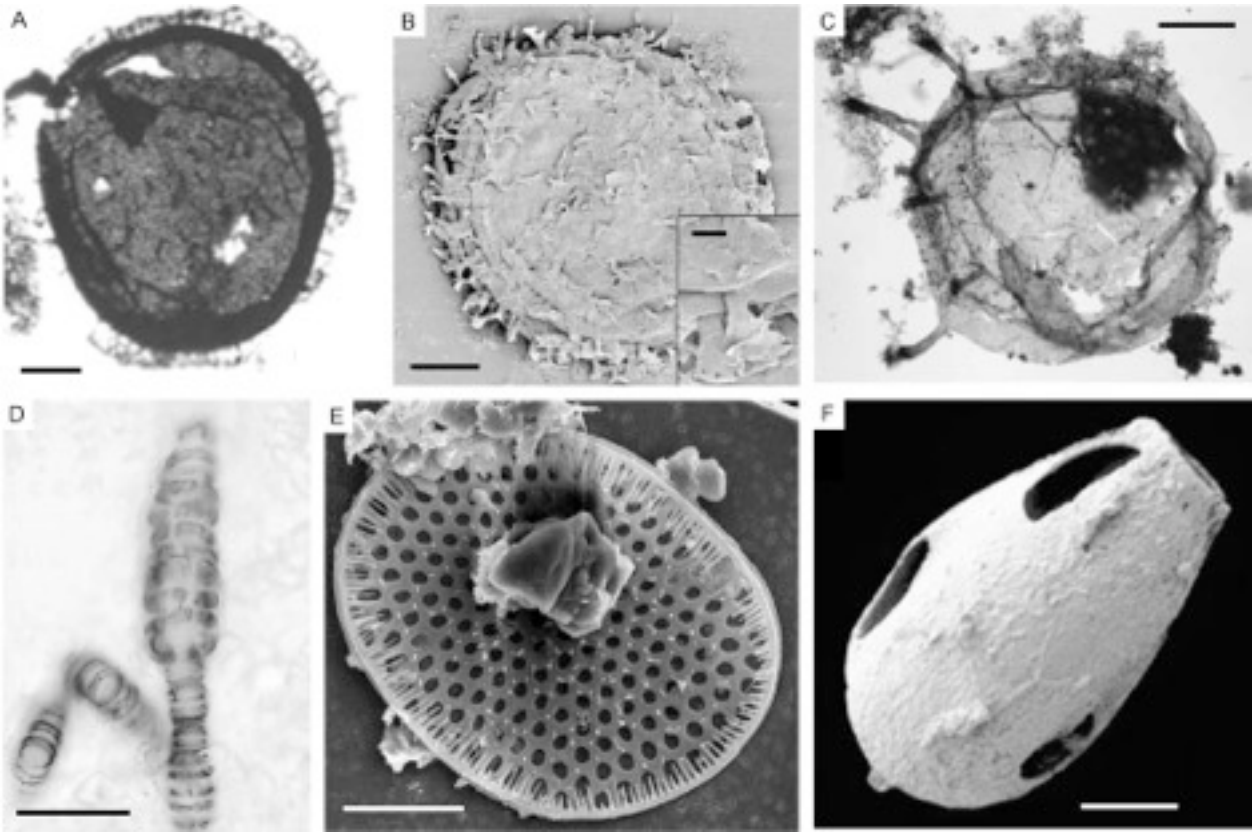

FIGURE *2*.—Proterozoic record of eukaryotic microfossils. (A, B) *Shuiyousphaeridium macroreticulatum* from the latest Paleoproterozoic Ruyang Group of China; A) light photomicrograph; B) SEM image. C) *Tappania plana* from the Mesoproterozoic Roper Group of Australia, with inset enlargement of external margin process. D) *Bangiomorpha pubescens* from the Mesoproterozoic Hunting Formation of Canada. E) *Thorakidictyon myriocanthum* from the Cryogenian Fifteenmile Group, Canada. F) Vase-shaped microfossil with potentially predation-mediated half-moon perforations from the Cryogenian Chuar Group, USA. Modified from: (A-B) Knoll et al., 2006; (C) Javaux et al., 2004; (D) Butterfield, 2000; (E) Cohen and Knoll, 2012; (F) Porter et al., 2003. Scale bar: A, B, D = 50 μm; B inset, E = 10 μm; C, F = 25 μm.

occur in the latest Paleoproterozoic–early Mesoproterozoic (ca. 1.8–1.6 Ga) Ruyang Group of China (He et al., 2009; Su et al., 2012; Pang et al., 2013, 2015) and the Mesoproterozoic (ca. 1.5 Ga) Roper Group of Australia (Javaux et al., 2004). These acritarchs, most notably *Shuiyousphaeridium macroreticulatum* and *Tappania plana,* as well as *Satka favosa* and *Valeria lophostriata*, are characterized by morphological complexity, large size, and encystment structures (Javaux et al., 2004). Occurrences of *Shuiyousphaeridium* (Fig. 2A, B) in the Ruyang Group are characterized by large size (up to 250 μm) and a highly ornamented, reticulated, and multi-layered wall composed of hexagonal plates and bearing external processes (Javaux et al., 2004). *Tappania*, which is also known from Mesoproterozoic successions of India and Russia, contains differentiated wall processes, potential budding and encystment structures, and may even represent a multicellular eukaryote (Fig. 2C; Javaux et al., 2001, 2004).

Roper Group and Ruyang Group *Valeria* are characterized by complex, concentric ornamentation (e.g., Pang et al., 2015), and the wall of *Satka favosa* (Roper Group) is composed of tessellated polygonal plates (Javaux et al., 2004). Macroscopic carbonaceous compressions of potentially eukaryotic affinity, such as *Grypania spiralis* and *Horodyskia moniliformis,* also occur in Mesoproterozoic successions of North America, China, and Western Australia (e.g., Grey and Williams, 1990; Walter et al., 1990; Knoll et al., 2006). *Bangiomorpha*, the oldest fossil for which multicellularity, as well as a eukaryotic affinity, is strongly supported, occurs in the mid-Mesoproterozoic (ca. 1.2 Ga) Hunting Formation of Canada (Butterfield, 2000). *Bangiomorpha pubescens* is characterized by large size (up to millimeter-scale) and strong

morphological differentiation, including a differentiated holdfast and uniseriate and multiseriate filaments, as well as radial division of discoidal cells (Fig. 2D). The various life-cycle stages indicated by *Bangiomorpha* assemblages suggest that it reproduced sexually (Butterfield, 2000). These features suggest a shared affinity with modern bangiomorphan red algae, supporting a Mesoproterozoic appearance for crown-group red algae (Butterfield, 2000; Knoll, 2014). There is also evidence for diverse eukaryotes in mid-Mesoproterozoic lacustrine deposits (e.g., Strother et al., 2009), raising the intriguing possibility that patterns of eukaryotic diversification in marine and terrestrial environments roughly mirrored each other.

Major radiations in eukaryote diversity are recorded in mid-Neoproterozoic microfossil assemblages of pre-glacial Cryogenian age (ca. 800 Ma; Fig. 1). Prominently, these radiations include the appearance of two major categories of eukaryotic microfossils: 1) the vase-shaped microfossils (VSMs; Fig. 2F), may be comparable to the tests of eukaryophagic testate amoebae (Knoll, 2014); and 2) phosphatized scale microfossils (Fig. 2E), may record phosphatic biomineralization, although a diagenetic origin for the phosophate has not been ruled out (Cohen and Knoll, 2012; Knoll, 2014). The appearance of these taxa ca. 800 Ma may reflect the emergence of eukaryophagy, in that resistant tests may have been an anti-predatory adaptation while also enhancing the preservation potential of the associated organisms (Porter et al., 2003; Porter, 2011; Knoll, 2014). The occurrence of half moon-shaped perforations (Fig. 2F) in VSMs of the Cryogenian Chuar Group of the western USA may also provide evidence for a Tonian appearance of eukaryophagy (Porter et al., 2003). This striking radiation in the diversity and biomechanical complexity of eukaryotic microfossils presages the much more dramatic eukaryotic radiations of the late Neoproterozoic and early Phanerozoic, and may indicate that ecological drivers were, in part, responsible for the 'slow fuse' to the metazoan radiations of the Ediacaran, Cambrian, and Ordovician.

The biomarker record holds the ability to shed unique light not only on the appearance of various eukaryotic clades but also to elucidate-specific constraints concerning the quantitative dominance of different groups within primary producing communities and the relative abundance of eukaryote versus prokaryote biomass inputs through geological time. Although very low organic compound concentrations, high thermal maturity, and contamination by exogenous organic matter have prompted concern regarding the validity of some Precambrian lipid biomarker studies, recently developed analytical techniques, such as analysis of the kerogen-bound pool, performed in parallel with analysis of free biomarker hydrocarbons, have placed new and rigorous constraints on the fidelity of Precambrian biomarker records (Love et al., 1995, 2009).

Evidence from lipid surveys of extant microorganisms, combined with genomic data (e.g., Volkman, 2003, 2005; Brocks and Pearson, 2005; Summons et al., 2006; Kodner et al., 2008) and temporal patterns of ancient steranes (fossil steroids) from Proterozoic (e.g., Summons and Walter, 1990; McCaffrey et al., 1994; Brocks et al., 2005; McKirdy et al., 2006; Grosjean et al., 2009; Love et al., 2009) and Phanerozoic successions (e.g., Grantham and Wakefield, 1988; Summons et al., 1992; Schwark and Empt, 2006) suggests that 24-alkylated steroids are robust markers for eukaryotes. In the Proterozoic rock record, microalgae are most likely a major source of these steranes. The most commonly biosynthesized steroids are the C_{27}, C_{28}, and C_{29} sterols, which are largely preserved over geologic time as C_{27}, C_{28}, and C_{29} steranes. The most abundant regular (4-desmethyl) sterane constituents of any particular Proterozoic rock or oil are either C_{27} or C_{29} compounds, and the relative proportion of C_{27} steranes (cholestanes) to total $C_{27\text{-}29}$ abundances can be interpreted to reflect the balance of red over green algal communities because red algal clades generally biosynthesize C_{27} sterols preferentially (Volkman, 2003; Kodner et al, 2008). As such, high relative abundance of C_{29} steranes (stigmastane) prior to the Paleozoic appearance of terrestrial plants reflects high green algal inputs (Volkman, 2003). C_{30} steranes occurring in Proterozoic sedimentary successions include: 1) dinosteranes (4α,23,24-trimethylcholestanes), whose sterol precursors are biosynthesized almost exclusively among modern organisms by dinoflagellate algae (Volkman, 2003); 2) 24-*n*-propylcholestanes from marine pelagophyte algae, which are ubiquitous in modern marine settings (Moldowan et al., 1990); and 3) 24-isopropylcholestanes, which are derived from sterols that comprise the major sterol constituents only in the Halichondrida order of demosponges, and thus can be used to track the appearance of early animals in the Proterozoic

sedimentary record (McCaffrey et al, 1994; Love et al., 2009, 2015).

Although extractable steranes have been previously reported from mature 1.7–1.3 Ga Paleoproterozoic and Mesoproterozoic successions from the Yanshan Basin in North China (e.g., Li et al., 2003) and from the 1.1 Ga Nonesuch Formation, USA (Pratt et al., 1991), these signals likely record late-stage contamination by anthropogenic fossil fuel sources. Recent reanalysis of putative Archean steranes and hopanes from the Pilbara Craton, Australia (French et al., 2015), and even analysis of thermally well-preserved and organic-rich Proterozoic strata of the 1.64 Ga Barney Creek Formation, Australia (Brocks et al., 2005), and the 1100 Ma Touirist Formation of Mauritania (Blumenberg et al., 2012), indicate that steranes in these successions are below detection limits and suggest that prior to the Neoproterozoic (>1 Ga), the absolute abundance of eukaryotes was low.

In contrast to earlier strata, both kerogen and bitumen extracted from the Cryogenian (ca. 740–800 Ma) Chuar Group contain notable abundances of polycyclic biomarker alkanes. particularly hopanes, steranes dominated by C_{27} compounds, and gammacerane. The presence of a genuine sterane signal in the Chuar Group, coupled with higher hopane/sterane ratios than the Phanerozoic average (0.5–2.0) for organic-rich rocks and oils, indicates a strong eukaryotic (and, in the case of C_{27} steranes, red algal) component to primary production that, importantly, was not necessarily eukaryote-dominated (Summons et al., 1988; Ventura et al., 2004). However, unambiguous evidence for extensive eukaryotic (i.e., algal) primary production is recorded in strata in South Oman, deposited during the interglacial interval of the Cryogenian (Love et al., 2009), with a C_{29} sterane predominance indicative of high green algal inputs. Moreover, the earliest biomarker record of metazoans, in the form of elevated amounts of 24-isopropylcholestanes (only abundant in a subset of demosponges), is also recorded in thermally well-preserved late Cryogenian strata from South Oman (Love et al., 2009, 2015). Sedimentary 24-isopropylcholestanes, the geological remnants of distinctive C_{30} sterols produced in abundance by certain genera of marine demosponges (McCaffrey et al., 1994; Love et al., 2009, 2015), have been recorded in significant quantities in all formations of the Huqf Supergoup of the South Oman Basin, and suggest that demosponges achieved ecological prominence in shallow-marine settings by the late Cryogenian. Although putative sponge-mediated carbonate textures have been described from Tonian and pre-Sturtian glacial reefal deposits (Neuweiler et al., 2009), these structures have not been linked conclusively to metazoans, and, on the basis of observation of similar textures associated with modern microbialites (Planavsky, 2009), a microbial origin may be possible. The earliest widely accepted record of poriferans therefore does not extend earlier than the interglacial Cryogenian demosponge biomarkers (Love et al., 2009) and late Ediacaran body fossils (Clites et al., 2012).

Although biomarker evidence for metazoans does not currently predate the Cryogenian interglacial interval, and body-and trace-fossil evidence for crown-group metazoans does not predate the earliest Cambrian and late Ediacaran, respectively (Jensen, 2003; Jensen et al., 2006; Erwin et al., 2011; Pecoits et al., 2012), molecular clock estimates place the LCA of metazoans in the pre-glacial interval of the mid-Cryogenian (ca. 800 Ma; Fig. 1). If the molecular clock estimates are correct, the development of the metazoan 'toolkit' and emergence of early crown-group animals preceded the current biomarker record and the body and trace fossil records by 100–250 million years. A pre-interglacial (and thus pre-demosponge biomarker record) origin for metazoans may be supported by recent work suggesting that ctenophores, rather than sponges, are the metazoan group closest to the metazoan LCA (Moroz et al., 2014; Whelan et al., 2015), which would in turn indicate a very early, or perhaps even basal, development for heterotrophy and predation within or even at the root of Metazoa.

If molecular estimates are accurate, a lag between molecular clock estimates and the biomarker, body, and trace-fossil records would suggest that taphonomic conditions—including, perhaps, size—were not sufficient for the preservation of the earliest metazoans. The Ediacara Biota, the first macrofossil assemblage containing indisputable metazoans (e.g., Jensen et al., 2003; Droser et al., 2006), is preserved worldwide in Konservat Lagerstätten of late Ediacaran age. These fossil assemblages are preserved in spite of the almost entirely soft-bodied composition (but see Clites et al., 2012) of Ediacara organisms. However, Ediacara fossils are typically macrofaunal (>1 mm) in scale; if earlier metazoans did not exceed the micro- or

meiofaunal scales, it is conceivable that taphonomic filters were not sufficiently fine to capture soft-bodied organisms of such diminutive scale. Alternatively, the earliest metazoans, particularly if they were of sub-macrofossil size, may not have been sufficiently morphologically differentiated from other non-metazoan (i.e., protistan) eukaryotes to be recognized as such. Alternatively, taphonomic windows responsible for preservation of Ediacaran macrofossils may not have been deeply rooted enough, temporally, to promote the fossilization of pre-Ediacaran metazoans.

REDOX PROXIES

There has been extensive work over the past decade on tracking the oxygenation of Earth's surface, and a coherent picture is emerging (e.g., Lyons et al., 2014). However, there is still debate over, and sizeable gaps in, understanding of several key aspects the rise of oxygen. Traditionally, it has been assumed that Earth underwent a unidirectional and protracted oxygenation with significant stepwise increases in oxygen levels at the beginning and end of the Proterozoic. Evidence for a jump in oxygen levels in the early Proterozoic is now well-established. This interval of oxygenation is typically referred to as the Great Oxidation Event (GOE), in spite of growing knowledge that this switch in Earth states was more likely to have been a gradual transition than a discrete event (Lyons et al., 2014). In contrast, the picture of redox evolution in the middle and late Proterozoic is rapidly evolving. Historically, Proterozoic oceans were thought to have become pervasively oxygenated after the last deposition of major Superior-type iron formation (IF) at ca. 1.85 Ga (Holland, 1973). This paradigm was challenged by Canfield (1998), who linked the end of IF deposition to the switch from anoxic and iron-rich (ferruginous) conditions to anoxic and sulfide-bearing (euxinic) conditions. In this model, aqueous sulfide (H_2S) scavenges iron, inhibiting iron transport and consequently shutting down IF deposition. The potential for a 'Canfield Ocean' initiated a new wave of research, but (as outlined below) additional work has not supported the community's initial interpretation of this model—that is, ubiquitous H_2S throughout the global deep ocean. Rather, building evidence indicates that ferruginous conditions were common in the mid-Proterozoic oceans with only limited extents of euxinia.

There is also growing support for the idea that the rise of oxygen following the GOE was not unidirectional, as traditionally envisioned. Geochemical evidence indicates that, following the GOE, a roughly 100 million-year shift to a more oxygenated Earth state (Planavsky et al., 2012; Partin et al., 2013a) occurred during Earth's largest positive carbonate-carbon isotope excursion (the 2.3–2.1 Ga Lomagundi Event; e.g., Karhu and Holland, 1996). Because the focus of this paper is on the billion years leading up to the onset of glacial conditions in the Neoproterozoic, we will not discuss the Lomagundi Event and the evidence for an alternative view to Earth's oxygenation—details in that regard are available elsewhere (e.g., Lyons et al., 2014). However, it is also possible that multiple rises and falls in surface oxygen levels of significant scale (spanning orders of magnitude) occurred throughout the Proterozoic, and that fluctuating oxygen concentrations were not a solely Paleoproterozoic phenomenon. Support for this possibility is presently limited. One potentially dramatic deviation from the traditional view of Proterozoic redox evolution with important implications for life is that very low (<<1% PAL) atmospheric oxygen concentrations may have prevailed intermittently during the mid-Proterozoic (Planavsky et al., 2014). Very low atmospheric oxygen concentrations during this interval would have resulted in poorly buffered atmospheric chemistry. Specifically, under low-oxygen conditions, small changes to the global carbon cycle (which is most closely tied to the global oxygen budget) would have induced disproportionately large changes in the percent of atmospheric oxygen.

Understanding Earth's oxygenation depends largely on geochemical tracers. These redox proxies can be grouped into two main categories: marine and atmospheric. At high atmospheric oxygen partial pressures, marine surface waters are typically close to equilibrium with the atmosphere. However, although the redox states of the ocean and atmosphere are tightly coupled, it is possible for a range of marine redox states to coexist under a narrow range of atmospheric oxygen concentrations. At low atmospheric oxygen levels, strong disequilibrium may exist between atmospheric and surface-ocean oxygen concentrations due to local oxygen production (Olson et al., 2013; Reinhard et al., 2013a). The broader marine redox landscape is controlled not

only by atmospheric oxygen levels, but is also strongly influenced by the location and temperature of water mass subduction, marine circulation dynamics, the extent of primary productivity, and the mechanisms and rates by which organic matter is exported from the photic zone. In this context, marine and atmospheric redox proxies are reviewed separately, recognizing that a comprehensive view requires integration of both proxy types. Furthermore, only a fraction of the redox proxies that have been used to track marine redox evolution are discussed below. In the spirit of keeping this discussion current, we have specifically chosen to emphasize recent and still-emerging proxies, which, over the past decade, have been employed extensively and have yielded significant insights into the processes and rates of Earth's redox evolution.

Using iron speciation to track ocean oxygenation

Iron (Fe) proxies, if applied properly, are one of the most robust tools available to track oxygen levels in the ancient oceans. These proxies are based on relationships between total Fe content (Fe_T) and iron sulfides (Fe_{SUL}), plus iron-rich, sulfide-reactive mineral phases such as oxides in fine-grained siliciclastic rocks—giving rise to the term "iron speciation." Iron bound in sulfides plus iron in phases in which it can react with H_2S on short diagenetic time scales is collectively known as highly reactive Fe (Fe_{HR}). The resulting paleoredox parameters are empirically based, but there is a firm understanding of the mechanistic and kinetic underpinnings of Fe speciation signatures (Poulton et al., 2004; Poulton and Canfield, 2005, 2011; Lyons and Severmann, 2006; Canfield et al., 2007, 2008; Johnston et al., 2010). Based on the framework developed from extensive work on modern sediments and in Phanerozoic sedimentary systems (where paleontological and organic geochemical records independently constrain redox conditions), ratios among the analytical iron parameters in sedimentary rocks can be used to elucidate past redox conditions. In short, ratios of Fe_{HR}/Fe_T exceeding the background siliciclastic flux (i.e., oxic marine sediments delivered principally by riverine processes) provide a signal for enhanced ferrous Fe transport under anoxic depositional conditions. If there is a signal for anoxic deposition, the ratio Fe_{SUL}/Fe_{HR} can then be used to establish whether the system was Fe(II)- or H_2S-buffered. An anoxic system with a relatively small amount of Fe_{HR} converted to pyrite indicates a depositional environment in which the reactive Fe supply was greater than the titrating capacity of available H_2S produced by microbial sulfate reduction, i/ e., a low Fe_{SUL}/Fe_{HR} ratio implies that sulfide was absent from both the water column and sediments. In contrast, a system with Fe_{HR} enrichments in which the vast majority of the highly reactive Fe has been converted to pyrite (high Fe_{SUL}/Fe_{HR}) is a signal for deposition under anoxic and sulfidic (euxinic) conditions.

A surge in Fe speciation work over the past decade has yielded important information about the redox structure and evolution of Earth's ancient oceans (see Poulton and Canfield, 2011; Lyons et al., 2014). One of the particularly significant conclusions to have emerged from these iron speciation studies is the idea that ferruginous (anoxic but non-sulfidic) marine conditions were likely a persistent condition throughout the Precambrian (Canfield et al., 2008; Planavsky et al., 2011; Poulton and Canfield, 2011; Lyons et al., 2014), in contrast to earlier arguments that limited such conditions mostly to the Archean. In particular, evidence is emerging for widespread ferruginous marine conditions between 1.7 and 0.7 Ga, which is accordingly reshaping the understanding of the evolution of global ocean chemistry. Buildup of ferrous iron in the water column can only occur when the rates of iron delivery to the water column exceed rates of water-column sulfate reduction. In spite of their rarity in anoxic regions of the modern ocean, ferruginous conditions were likely common in the Proterozoic global ocean, due, in part, to low (likely μM or low mM) marine sulfate concentrations. For example, low marine sulfate concentrations in theory could have allowed for larger iron fluxes from terrigenous sediments and from hydrothermal systems. It is unlikely, however, based on the extent of oxidant consumption in the modern oceans, that sulfate concentrations were too low to sustain microbial sulfate reduction. It is more likely that organic matter loading in marine systems played an important role in controlling the distribution and extent of ferruginous conditions, and the local development of euxinic conditions would have been limited by the intensity of organic matter loading and associated sulfate reduction by microbes that use that organic matter as an electron donor. Regardless of the cause, extensive anoxic and ferruginous conditions likely prevailed through much of the mid-Proterozoic (Canfield et

al., 2008; Planavsky et al., 2011; Poulton and Canfield, 2011).

It is important to keep in mind that much of this work has been developed in the absence of a detailed petrographic context and specifically without stringent filters for rock types suitable for Fe speciation. Furthermore, our extraction schemes for Fe speciation and the associated threshold values should be subjected to frequent scrutiny, including consideration of the complications associated with burial and concomitant mineralogical alternation. Although Fe speciation provides a robust means to track local redox conditions, extrapolations to large-scale conditions require caution. Therefore, Fe proxies are ideally employed when coupled with other geochemical tracers and approaches, such as novel isotope techniques and numerical modeling, that help shed light on global rather than local redox conditions.

Using trace-metal enrichments and isotope values to track ocean oxygenation

Trace-metal enrichments in black shales can record information about the global ocean redox state. The size of the global marine reservoir of redox-sensitive elements (RSEs) is primarily controlled by the balance between the spatial extent of anoxic versus oxic waters in marine environments. This relationship is underpinned by the simple premise that the burial rates of many redox-sensitive elements (e.g., Mo, V, Re, Cr, and U) are much higher in sediments deposited under anoxic water-column conditions as compared to those deposited in well-oxygenated settings (Emerson and Huested, 1991; Scott et al., 2008). For example, molybdenum is the most abundant transition element in modern oceans (with a seawater concentration of ~107 nM), despite being a very minor component of the continental crust (~1 ppm). This disparity is a direct result of the modern marine redox state— modern oceans are largely oxic, and Mo is extremely soluble in oxygenated waters. Euxinic (anoxic and sulfidic) water column and suboxic sediments with sulfidic pore waters, environments where Mo is preferentially buried, are spatially limited in the modern oceans, allowing Mo to accumulate to its present concentration in seawater (e.g., Emerson and Huested, 1991). Therefore, a more limited distribution of reducing conditions in the ocean leads to a concomitantly larger marine reservoir of RSEs.

Redox-sensitive trace-metal enrichments can be used to track global ocean oxygenation, as the magnitude of a given RSE enrichment in anoxic marine sediments is generally characterized by a first-order scaling to its dissolved concentration in seawater. In other words, a higher mean dissolved concentration of a given trace element will result in a greater enrichment in anoxic sediments. Because the dissolved concentrations of redox-sensitive trace metals will be controlled by the marine redox landscape (as discussed above), local trace-metal enrichments in sediments deposited in anoxic settings can track global redox conditions. Therefore, the large sediment trace metal enrichments observed in, for example, the modern anoxic Cariaco basin are the direct result of local anoxia, but they also provide a signal that anoxia on a global scale is extremely limited today. A key aspect of using the magnitude of trace-metal enrichments to track global marine redox evolution is using an additional, independent redox proxy to determine local water-column redox conditions. Sediments of local anoxic subenvironments will become enriched in metals at a level proportional to the marine inventory of that metal, and thus the global distribution of anoxia. Broad global anoxia means lower local enrichment. As discussed above, Fe speciation provides a rigorous means to access those local paleoredox conditions. It is important to note that this framework does not apply to settings characterized by oscillatory redox conditions (e.g., settings in which periodic 'burndown' occurs during oxic intervals).

There have been several attempts to provide a record of trace-metal enrichments in anoxic shales through time (Emerson and Huested, 1991; Scott et al., 2008; Sahoo et al., 2012; Partin et al., 2013a, b; Reinhard et al., 2013b). Relative to modern anoxic basins with a strong marine connection (i.e., not fully restricted) and to Phanerozoic averages for anoxic shale values, Mo, U, and Cr enrichments are consistently low in anoxic shales deposited from 1.8 to 0.8 Ga. A jump in trace-metal enrichments in the Neoproterozoic provides one of the most compelling lines of evidence for a late Precambrian (Fig. 3) oxygenation event (Lyons et al., 2014). There is strong evidence for a short-lived increase in the magnitude of trace metal enrichments (e.g., V, Mo, U, and Cr) following the second of the 'Snowball Earth' glacials—the ca. 635 Ma Marinoan glaciation. Enrichments in these Ediacaran-aged shales are close to the anoxic Phanerozoic mean and are larger than

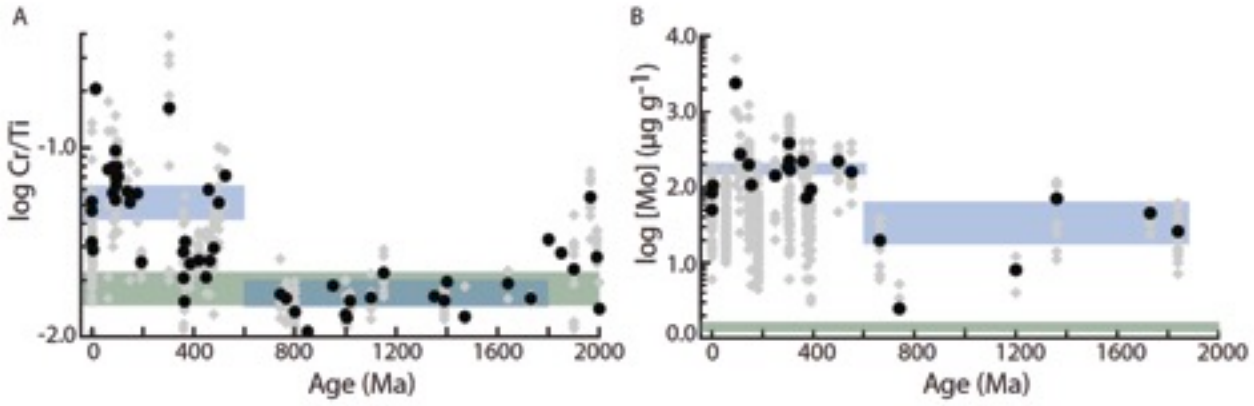

FIGURE *3*.—Trace metal records of evolving ocean redox during the mid-Proterozoic. Data have been filtered by independent methods to represent anoxic (A) and euxinic (anoxic and sulphidic) (B) marine environments. Green boxes represent the range for upper continental crust. Blue boxes denote the average values for mid-Proterozoic and Phanerozoic data. Black (filled) circles represent unit mean values. Large Phanerozoic Cr and Mo enrichments point to a dominantly oxic ocean (with low enrichments being linked predominantly to anoxic events or severe isolation). Large Cr enrichments in the early Proterozoic similarly suggest a well-oxygenated ocean, while persistently muted Cr enrichments in the mid-Proterozoic suggest reversion back to a poorly ventilated ocean. Modest Mo enrichments in the mid-Proterozoic, however, suggest that only a moderate extent of this poorly oxygenated ocean was euxinic. After Reinhard et al. (2013b).

those observed in the modern Cariaco Basin. Trace-metal enrichments from the Ediacaran of South China provide clear evidence for a well-oxygenated ocean-atmosphere system (Sahoo et al., 2012). Large Mo, Cr, and U enrichments (well above the Proterozoic mean) were reported from the ca. 800 Ga Wynniatt Formation in the Shaler Supergroup (Thomson et al., 2014). These enrichments provide evidence for a shift to a more oxygenated ocean-atmosphere system well before the onset of widespread glaciation.

One of the appeals of using RSE enrichments to track ocean oxygenation is that this approach yields quantitative estimates (e.g., areal extent) of seafloor redox conditions. This methodology builds directly from modern global marine metal mass-balances and work on metal enrichments in Cenozoic foraminifera (Hastings et al., 1996). Reinhard et al. (2013b) and Partin et al. (2013a) provided the most recent reconstructions of the Proterozoic marine redox landscape using this approach, and suggested that the Proterozoic ocean until ca. 800 Ma was pervasively anoxic (≥40–50% of Proterozoic seafloor area, and potentially substantially higher) relative to Phanerozoic conditions, but was characterized by a relatively limited extent of euxinic seafloor conditions (<1–10% of modern seafloor area), which is still large compared to the <<1% observed today.

The seawater Mo isotope composition provides addition global perspective because it is controlled by the extent of Mo burial under oxic, suboxic, and euxinic conditions. Oxic and suboxic environments preferentially bury isotopically light Mo, which drives the dissolved seawater to heavier δ^{98}Mo values. In contrast, it is typically thought that there is more limited fractionation during Mo burial in euxinic environments (Arnold et al., 2004). In this framework, seawater δ^{98}Mo values can be used to estimate the extent of euxinic environments on a global scale. Furthermore, euxinic shales can come close to capturing the coeval seawater δ^{98}Mo, as seen in the Black Sea today. As such, if independently constrained by Fe speciation as euxinic, local shales can provide a window to global conditions. Accordingly, heavy Mo isotope values in euxinic shales have been used as evidence for relatively limited euxinia (as seen today), and light values, those near the composition of the crust, have been used as evidence for widespread euxinia. There are, however, a few complications to this story. Foremost, since this framework was first proposed, it has become clear that euxinic shales do not always capture seawater values (e.g., Noordmann et al., 2015). This observation demands refinements to the global isotope mass balance but, most importantly, it means that care must be taken when interpreting Mo isotope data from euxinic shales. With this in mind, it is difficult to use Mo isotope values to quantify the

extent of euxinic conditions beyond useful approximations. However, the current Mo isotope record (albeit limited) for the mid-Proterozoic suggests a greater extent of shallow-ocean euxinia than that observed in the modern oceans, but is incompatible with widespread euxinia in the deep oceans. In this regard, the Mo isotope record is in close agreement with constraints offered by the metal enrichment records and indicates that, on a global scale, euxinia was limited in the mid-Proterozoic ocean and was confined to regions of locally high-organic matter loading.

Using sulfur isotopes to track ocean oxygenation

Sulfur (S) isotopes provide a natural complement to the bulk Fe-S-C, RSE, and Mo isotope chemistry of sedimentary rocks, and, when combined, these systems can provide strong constraints on local redox conditions as well as information about global ocean redox chemistry. Microbial sulfate reduction induces a significant kinetic isotope effect, causing depletion in $\delta^{34}S$ values, relative to the initial seawater sulfate $\delta^{34}S$ composition for sulfide phases formed in the water column and/or sediments. Microbial sulfate reduction in sulfate-depleted systems results in an isotopic distillation effect, whereby the sulfide produced through this process becomes progressively heavier and ultimately can match the original seawater sulfate $\delta^{34}S$ signature, despite potentially large instantaneous fractionations during sulfate reduction (e.g., Gomes and Hurtgen, 2015). Thus, large fractionations tend to record relatively large sulfate availability, which is tied to both local redox chemistry (e.g., water-column versus diagenetic pyrite formation and connectedness of the system with the open ocean) and global sulfur cycling (the prevailing atmosphere-ocean redox state and attendant delivery of sulfate to the ocean as balanced by burial as either pyrite or sulfate evaporites).

The 1990s and early 2000s produced an extensive amount of work on the geological record of sulfur isotopes (Canfield and Raiswell, 1999; Johnston, 2011). With this surge of work came the expectation that constraining the ancient sulfur cycle was one of the best means available to track the redox state of Earth's surface. Accordingly, S isotopes were commonly used to track the size of the marine sulfate reservoir. The development of rare S isotope systematics (e.g., $\Delta^{33}S$) during this time also increased the resolving power of S isotopes (e.g., Johnston et al., 2007; Johnston, 2011). Over the past ten years, there has been an upswing in the number of experimental investigations of sulfur isotope behavior as well as actualistic studies grounded in observation of modern systems. Although experimental work has undoubtedly improved the understanding of the mechanisms driving sulfur isotope variation, an initial impression might indicate that this work has also clouded some of the central conclusions that can be drawn from S isotopes. For example, experimental work has bolstered the case that the isotopic fractionation that occurs during microbial sulfate reduction is strongly influenced by the rate of sulfate reduction, which challenges attempts to link geologic S isotope signatures to particular aqueous sulfate levels (Sim et al., 2011; Leavitt et al., 2013). However, one path forward might lie in a refined focus on euxinic settings, where pyrite formation occurs in the water column instead of in the sediment pile. In this case, rates of sulfate reduction will be subject to greater local variability (Scott et al., 2014; Gomes and Hurtgen, 2015). Sulfur isotope data from modern, low-sulfate euxinic systems illustrate that $\Delta^{34}S$ (the difference between sulfate and sulfide $\delta^{34}S$) values are positively correlated with aqueous sulfate concentrations (Gomes and Hurtgen, 2015). In other words, $\Delta^{34}S$ values in these systems are observed to increase with sulfate concentration. Euxinic settings recorded in mid-Proterozoic successions are characterized by a limited range of isotopic variation (low $\Delta^{34}S$), providing strong evidence for persistently low marine sulfate concentrations (Scott et al., 2014). This conclusion is consistent with most other constraints on contemporaneous sulfur cycling. Low marine sulfate concentrations are best explained by a marine system with extensive anoxia and limited sulfide re-oxidation (i.e., efficient burial as pyrite). It has been proposed that low Proterozoic marine sulfate levels could be caused by inhibited sulfide oxidation during weathering. However, this seems unlikely considering typical denudation timescales compared to the very rapid rates characterizing sulfide oxidation at even the lowest estimates of Proterozoic oxygen partial pressures (e.g., Reinhard et al., 2013a).

The first occurrence of sulfides in euxinic shales with $\Delta^{34}S$ values near the maximum fractionations observed in modern cultures ($\Delta^{34}S$ >60‰) occur in ca. 800 Ma successions (Fig. 4). This increase in $\Delta^{34}S$ is roughly synchronous with

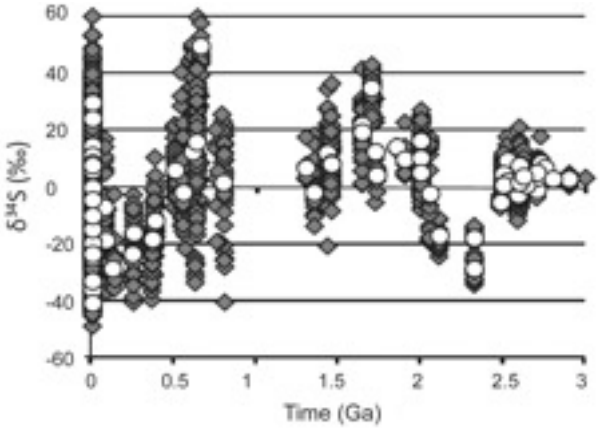

FIGURE *4*.—A compilation of pyrite sulfur isotope data through time from organic-rich shales. A large portion of these units are from euxinic shales (see Scott et al., 2014). There is a marked increase in the range of sulfur isotope values in the Neoproterozoic. Gray diamonds are individual bulk sample measurements, white circles indicate formation means. Modified from Scott et al. (2014).

notable increases in the volume of sulfate evaporite deposition, as recorded in the Centralian Superbasin successions in Australia, and the Shaler Supergroup in Canada. These shifts in the S cycle are also stratigraphically proximal to the first occurrence of black shales containing trace-metal enrichments (Mo, V, Cr, U) that are comparable to those recorded in modern (e.g., Cariaco Basin) euxinic sediments (Thompson et al., 2014). In summary, constraints from the sulfur cycle can offer a wide range of insights into Proterozoic biogeochemical cycling. Most importantly, however, they provide additional support for a significant shift in marine redox conditions around 800 Ma.

TRACKING ATMOSPHERIC OXYGENATION

Although there is a suite of proxies that can be used to track marine redox evolution, only a limited number of proxies can be employed to track atmospheric oxygen levels. Traditionally, tracking redox reactions in paleosols has been the chief means of estimating Proterozoic atmospheric oxygen levels. Paleosols provide the ideal medium for tracking atmospheric oxygen levels, given that, as terrestrial deposits, they may directly record the chemical byproducts of interaction with atmospheric oxygen. However, the identification of Proterozoic paleosols (hundreds of millions of years prior to the evolution of land plants) is challenging (Tarhan et al., 2015). Unsurprisingly, there is a dearth of undisputed Proterozoic paleosols, and work on these putative paleosols has proven to be controversial. Exacerbating this uncertainty, current paleosol records have largely failed to provide a coherent picture of mid-Proterozoic atmospheric oxygen levels. Driese at al. (1995) reported evidence for the oxidation of manganese (Mn) and Fe in paleosols hosted by the 1.75 Ga Lochness Formation in northern Australia. Pan and Stauffer (2000) found a positive Ce anomaly, with the presence of cerianite, in a 1.85 Ga paleosol at Flin Flon, Manitoba, Canada, which was taken to indicate that atmospheric pO_2 was $\geq 10^{-1.5}$ to 10^{-2} present atmospheric levels (PAL). However, more recent work has uncovered no evidence for Mn redox cycling in those paleosols, indicating that contemporaneous oxygen levels may not have exceeded 10^{-2} PAL. There appears to be Mn loss but Fe retention in the ca. 1.7 Ga Baraboo paleosol of Wisconsin, USA (Driese and Medaris, 2008). Initial surveys suggested that the 1.1 Ga Sturgeon Falls paleosol in the mid-continent rift succession of Michigan, USA (Zbinden et al., 1988) was also characterized by Mn loss. More in-depth work on a suite of paleosols preserved in the mid-continent rift succession of the Superior region (Mitchell and Sheldon, 2010; Sheldon, 2013) confirmed loss of Mn and additionally suggested loss of Fe. Additionally, this work on the exceptionally preserved paleosols of the Superior mid-continent rift succession provides support for the presence of low pCO_2 (i.e., within Cenozoic range) and low atmospheric oxygen concentrations (Mitchell and Sheldon, 2010; Sheldon, 2013). In sum, the paleosol record is consistent with a wide range of atmospheric oxygen levels through the mid-Proterozoic, potentially including very low surface oxygen levels. However, one of the most striking aspects of the record is the intriguing lack of definitive (cf. Rye and Holland, 1999) paleosols from roughly 1.7 to 1.1 Ga and from 1.0 to 0.7 Ga.

Chromium (Cr) isotope data provide an alternative means to track atmospheric oxygen levels. Redox reactions control the modern Cr cycle, and the initial stage of Cr redox cycling occurs almost exclusively in terrestrial environments, which sets the stage for using Cr isotopes to track atmospheric redox evolution independent of marine estimates. In igneous

rocks, Cr is present almost exclusively in the reduced [Cr(III)] form, which is readily oxidized in soil environments to Cr(VI) via surface interaction with Mn oxide phases (e.g., Fendorf, 1995). This process results in the formation of extremely soluble (and thus mobile) chromate species, predominantly CrO_4^{2-}. Importantly, this process is considered to proceed mainly through interaction of dissolved Cr(III) with solid-phase Mn oxides. Given the strong (low) pH dependency of Cr(III) solubility, this reaction is unlikely to occur at a marine pH, and instead occurs almost exclusively in terrestrial settings. In terrestrial settings, rainwaters, sulfide oxidation, and organic matter respiration all provide a source of acidity. Terrestrial chromate is by far the dominant source of Cr to the modern oceans (Rauch and Pacyna, 2009), and Cr is stable and largely conservative within oxygenated oceans. This generally conservative behavior is in contrast to that observed under anoxic conditions, where Cr(VI) is rapidly reduced by aqueous Fe(II) and sulfide, as well as by solid-phase reduced Fe and S and even some organic compounds (Richard and Bourg, 1991; Fendorf, 1995; Graham and Bouwer, 2010).

The Cr isotope system is unique in that the isotope composition of Cr in low-temperature rocks is controlled almost exclusively by redox transformations (Johnson and Bullen, 2004). There is a narrow range of Cr isotope values (reported as $\delta^{53}Cr$) in igneous systems, with an average value of -0.12‰ (± 0.1 2SD) (Schoenberg et al., 2008). Because Cr is present in igneous rocks exclusively as Cr(III), the initial Cr reservoir for terrestrial weathering will be stable under reducing conditions. Both theoretical and experimental studies indicate that Cr will undergo limited fractionation during non-redox-dependent transformations (Ellis et al., 2004; Johnson and Bullen, 2004; Schauble et al., 2004), as indicated by the common occurrence of sedimentary rocks with authigenic Cr enrichments that have crustal or near-crustal Cr isotope compositions (e.g., Frei et al., 2009).

In marked contrast to non-redox processes, oxidation and reduction of Cr induces large isotope fractionations. At equilibrium, the $Cr(VI)O_4^{2-}$ anion will be enriched by >6‰ relative to the parent Cr(III) reservoir (Schauble et al., 2004), although this full equilibrium fractionation is unlikely to be expressed (e.g., Zink et al., 2010). Kinetic fractionations between Cr(VI) and Cr(III) during reduction are typical in natural systems, and range between 3.0 and 5.5‰ (Ellis et al., 2002; Ellis and Johnson, 2004; Johnson and Bullen, 2004; Schauble et al., 2004; Zink et al., 2010). Thus, the redox cycling of Cr as initiated by oxidative Mn cycling in terrestrial settings will lead to large Cr isotope fractionations, and this fractionated Cr reservoir can be captured in terrestrial and shallow-marine sediments. In sum, Cr isotopes are ideally suited to track redox processes. Most importantly, because Cr redox cycling is intimately linked to the oxidative cycling of Mn in terrestrial environments, the Cr isotope system is uniquely suited to tracking atmospheric oxygenation.

Iron formations have played a crucial role in reconstructing a geologic Cr isotope record, following from the premise that as chemicals precipitate, they should trap an authigenic Cr isotope signal. The simplest interpretation of Cr isotope data in iron formation, building from the framework outlined above, is that crustal values indicate a lack of Cr redox cycling in terrestrial settings, leading to limited Cr mobility (and limited delivery of Cr to the oceans) and a mobile Cr load dominated by Cr(III). Somewhat surprisingly, our initial research has found that lower and middle Proterozoic iron formations and ironstones are characterized by limited Cr isotope variability (Fig. 5), despite containing Cr enrichments (Planavsky et al., 2014). Laser ablation work has confirmed that the Cr in these units is present in authigenic iron phases (e.g., iron granules and iron ooids) instead of in detrital chromite (Fig. 5B), providing strong support that these values record the behavior of the mobile Cr reservoir.

We have also been examining the shale Cr isotope record. Although shales commonly contain a significant detrital Cr load, reducing marine and terrestrial sediments can also develop large authigenic Cr enrichments. In a system characterized by active Cr redox cycling, both authigenic Cr and bulk sediments (detrital plus authigenic) should be characterized by Cr isotope variability. Interestingly, a survey of shales (N>250) indicated limited Cr isotope variation in Proterozoic sediments but large variations in Cenozoic shales characterized by Cr enrichments, comparable to those recorded in Proterozoic successions (based on Cr/Ti ratios; Planavsky et al., 2014; Cole et al., 2015). These results support previous observations based on Cr isotope data from iron formations, and suggest limited Cr redox cycling for at least intervals of the mid-

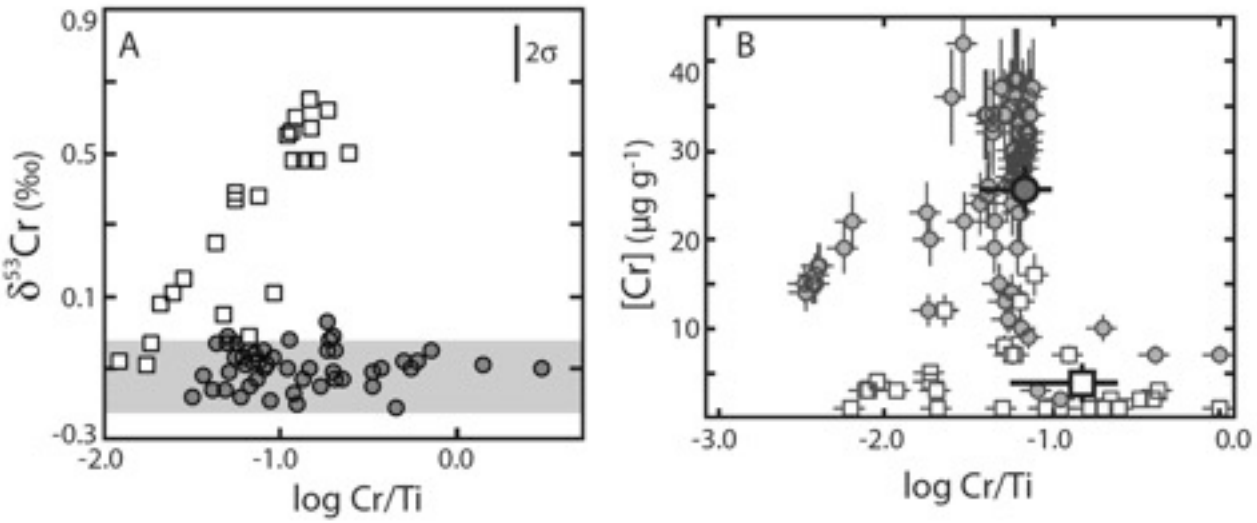

FIGURE 5.—A) Phanerozoic (white squares) and Proterozoic (circles) ironstones. The gray bar demarcates the igneous Cr isotope range, while the error bar in the top right denotes uniform external reproducibility (2σ). Phanerozoic and Proterozoic samples show a similar range in Cr/Ti ratios but markedly different Cr isotope trajectories. The trend defined by the Phanerozoic results from mixing between a crustal and a ^{53}Cr-enriched authigenic Cr component, providing a clear signal for an oxidative Cr cycle. B) In situ Cr and Ti concentrations for representative mid-Proterozoic ironstones. Hematitic sedimentary grains are shown as gray circles; hematite cements as white squares. Error bars in (B) denote uncertainty in measured concentrations of 15%, propagated into calculated Cr/Ti values. Large filled points denote the average values (±95% confidence interval) for grains (circles) and cements (white squares). After Planavsky et al. (2014).

Proterozoic.

Based on our current sample set, we observed a marked increase in Cr isotope variability between deposition of the ca. 850 Ma Aok ironstone and the ca. 900 Ma Wyniatt Formation in the Shaler Supergroup. This increase in Cr isotope variability occurs in a unit that is characterized by markedly light sulfur isotope values and large Mo enrichments. These results open up the intriguing possibility that a significant atmospheric oxygenation event preceded the Sturtian glaciation. However, evidence of significant Cr redox cycling is also reported from ca. 1 Ga carbonates (Bekker, 2015). These results might suggest that, against a backdrop of oxygen levels sufficiently high to induce active coupled Mn-Cr redox cycling, Proterozoic atmospheric oxygen levels were variable. As mentioned above, we would predict large-scale (orders or magnitude) variations in pO_2 values during the Proterozoic, given the greater capacity for fluctuation in oxygen concentrations possible with a smaller atmospheric oxygen reservoir. Importantly, these carbonate data are still consistent with low but variable oxygen levels in the Proterozoic atmosphere, and may capture the level of expected variability. However, given that it is difficult to preserve metal isotope signatures in carbonates, these results would ideally be validated by another geological archive.

One of the key remaining questions for Cr cycling is the question of exactly how much oxygen is needed to induce Cr isotope fractionations. This is a topic of active investigation currently being explored through experimental work and reaction transport modeling. However, a reasonable (and likely conservative) view would be that pO_2 values of $<10^{-3}$ PAL would be adequate to fuel active Cr-Mn cycling (Planavsky et al., 2014). This threshold is significantly lower than traditional estimates for Proterozoic atmospheric oxygen (0.01 to 0.1 PAL). However, as discussed above, previous minimum estimates are largely based on the sparse and contentious mid-Proterozoic paleosol record and are therefore tenuous (see also Lyons et al., 2014).

PROXY RECORD RELIABILITY

Chemical proxies (e.g., δ^{56}Fe, δ^{53}Cr, $\delta^{97/95}$Mo, δ^{34}S, Δ^{33}S, δ^{66}Zn, ^{87}Sr/^{86}Sr, ^{238}U/^{235}U, δ^{44}Ca, δ^{26}Mg, δ^{11}B, δ^{13}C, δ^{18}O, REE) are routinely measured in Precambrian geologic samples in order to reconstruct ancient marine and atmospheric conditions. However, there is

growing concern that bulk-rock geochemical signals may not be syngenetic, and that current methods are inadequate to detect diagenetic alteration in deep-time samples (e.g., Kirschvink et al., 2012; Pufahl and Hiatt, 2012). The preservation of primary geochemical signals has large implications for accurate reconstruction of Precambrian marine and atmospheric conditions, as efforts to date have been largely reliant on a geochemical toolkit. The problem is, in part, a classic Catch-22, as the ability to predict the operation of Precambrian diagenetic processes is to a large extent reliant upon understanding the chemistry of the Precambrian oceans. In addition, the ability to measure geochemical quantities is fast outstripping understanding of the systems they record (Watson, 2008). As analytical methods improve and researchers begin to explore previously elusive aspects of Precambrian geochemistry, distinguishing between depositional and secondary signals will be crucial in establishing reliable constrains on attempted environmental reconstructions. Increasingly rigorous standards will need to be met to demonstrate sample preservation and reproducibility, necessitating a multi-proxy approach.

Recent paleoredox work attempting to piece together the evolution of atmospheric and marine oxygen has focused on metal isotopes, often combining multiple isotope systems in order to better constrain the interaction of local- and global-scale processes, and replicate records across a range of depositional settings (e.g., Kendall et al., 2009; Planavsky et al., 2014; Auerbach et al., 2015). To date, however, limited efforts have been dedicated to verifying whether these proxies reliably record seawater values (see Pufahl and Hiatt, 2012, for a review). Organic-rich shales and iron formations have been the primary lithologies targeted, as they record marine chemistry within authigenic phases in addition to detrital minerals. Seawater composition is measured by assuming that the authigenic fraction captures water-column conditions and that it acts as a closed system after deposition. Secondary authigenic mineral formation during early diagenesis and lithification, as well as later-stage cation exchange with migrating fluids, will shift the composition of the authigenic phases away from primary seawater values. Bulk-rock measurements remain the only means available to measure most paleoredox proxies; samples with any obvious secondary alteration are discarded, but the boundary between well-preserved and altered samples can be poorly defined. Detailed petrographic work can be used to determine the origin of authigenic minerals; for instance, sulfides and oxides formed in seawater are characterized by distinct petrographic textures and thus trace metals hosted within these phases can be reliably interpreted to record seawater signatures. In addition, in-situ laser ablation measurements on authigenic minerals should show trace-metal enrichments above those of background detrital minerals, which will confirm their authigenic origin (e.g., Large et al., 2014). In addition to petrographic work, the recent refinement of radiogenic isotope systems presents the opportunity to use absolute age constraints to determine whether a geochemical system has experienced any addition or loss of elements of interest. Given the geochemical similarity between Re, Os, and most redox-sensitive metals of interest (e.g., Mo), Re-Os isochrons can be used to determine whether a system has remained closed since deposition by comparing it with an external age constraint (e.g., Anbar et al., 2007; Kendall et al., 2009). Any alteration will reset the Re-Os isochron and yield an erroneous age. Combined, these measures will help validate the primary origin of target mineral phases and ensure they were conserved after deposition.

Carbonates have been targeted for a much greater range of proxy-based assessments due to their widespread occurrence across Mesoproterozoic and Neoproterozoic successions (see Kah et al., 1999; Halverson et al., 2010). Moreover, carbonates incorporate a large range of elements during precipitation with minimal fractionation; thus, numerous isotope systems can be used to reconstruct seawater values from these lithologies (e.g., Palmer and Edmonds, 1989; Marriot et al., 2004). However, many carbonates are far more susceptible to diagenetic alteration than ironstones or shales due to their greater porosity and, in the case of certain carbonate mineralogies, their thermodynamic instability (Morse et al., 1985). In addition, typical marine carbonates contain, on average, up to ten percent detrital non-carbonate minerals, and have been subjected to diagenetic alteration, which results in cation exchange with both migrating fluids and non-carbonate minerals (Brand and Veizer, 1980; Bailey et al., 2000). Traditional carbonate carbon isotopes ($\delta^{13}C$) may remain largely unaffected, as carbon forms a dominant component of carbonate

mineralogy. Questions regarding the robustness of carbon isotopes generally center on a handful of sections with highly anomalous carbon isotope values (e.g., the Shuram-Wonoka excursion and the Bitter Springs anomaly; Knauth and Kennedy, 2009; Derry, 2010; Schrag et al., 2013). Interestingly, however, careful tests of the consistency of $\delta^{13}C$ and $\delta^{18}O$ measurements on clast assemblages from Shuram-penecontemporaneous carbonate breccias and across multiple stratigraphic sections demonstrate, in the case of the Shuram-Wonoka excursion, a depositional or early diagenetic signal for those anomalous values (Husson et al., 2012, 2015). The general consensus is that the Proterozoic carbon isotope record generally reflects global seawater values (Halverson et al., 2010). Unlike carbon isotopes, analysis of carbonate-hosted trace element isotopes have been much more problematic, both in regards to trace-element concentrations and isotopic values. To use the example of strontium isotopes ($^{87}Sr/^{86}Sr$), a radiogenic isotope system commonly used as a metric for weathering rates (MacArthur et al., 2012), Sr contamination can originate during diagenetic alteration of carbonate phases by Sr exchange from fluids and detrital phases into carbonate minerals, as well as during sample preparation by dissolving Sr-bearing detrital minerals in addition to the targeted authigenic carbonate minerals (Bailey et al., 2000; Brand et al., 2012). Contamination by detrital phases can be addressed by using a more comprehensive leaching method to both identify and limit detrital material contamination during sample preparation (Brand et al., 2012; Liu et al., 2014), yet differentiating between primary and secondary signals in the carbonate phases themselves has proven more challenging. Many workers employ alteration metrics developed for Phanerozoic carbonates (e.g., Kah et al., 2007). Unfortunately, these techniques assume an oxic marine depositional environment and a primary mineralogy of calcite and aragonite, whereas these conditions likely differed during the Proterozoic (Halverson et al., 2007; Hood et al., 2015). In addition to $^{87}Sr/^{86}Sr$, recent advances in geochemical methods have fostered the development of additional isotope proxy systems, such as $\delta^{11}B$ as a paleo-pH proxy (e.g., Ohnemueller et al., 2014); $\delta^{7}Li$ to measure weathering intensity (e.g., Pogge von Strandmann et al., 2014); $\delta^{66}Zn$ as a paleoproductivity proxy (Kunzmann et al. 2013); and, most recently, $\delta^{53}Cr$ to augment the shale chromium record of global redox cycling (e.g., Bekker, 2015). These emerging systems may answer many outstanding questions regarding the evolution of Precambrian environments, but they have yet to be fully scrutinized for their sensitivity to alteration, and tracers have not been developed to validate their primary origin.

NUTRIENTS IN THE PRECAMBRIAN OCEANS

Life in the oceans is limited by nutrient availability. Therefore, to track the evolution of the carbon cycle and emergence of modern-style redox processes, it is essential to understand the evolution of nutrient cycling. In most modern aquatic systems, primary production is limited largely by either phosphorus or nitrogen, or both (e.g., Howarth, 1988). Due to the virtually limitless supply of nitrogen supplied to the marine biosphere via fixation of atmospheric N_2, which buffers against temporally extended imbalances in fixed nitrogen availability, and the observation that phosphorus is sourced from continental materials and thus is of limited supply in the open oceans, phosphorus typically is considered to be the nutrient ultimately limiting net primary productivity on geologic timescales (Redfield, 1934; Tyrrell, 1999).

There are few proxies that are useful for the estimation of marine phosphate concentrations. The bulk P/Fe ratio of iron oxide-rich rocks is the only such proxy to have been extensively explored for Precambrian rocks. Iron-rich rocks have the potential to track the size of the marine phosphate reservoir through time if reasonable assumptions are made concerning P sorption behavior to iron oxides as well as the diagenetic history of a succession. Armed with these assumptions, these ratios can be used to determine the evolution of marine P concentrations through time (Bjerrum and Canfield, 2002; Konhauser et al., 2007). Bjerrum and Canfield (2002) proposed that the low P/Fe ratios (relative to Phanerozoic hydrothermal deposits) recorded in Archean and Paleoproterozoic iron formations provided a signal for extremely low seawater phosphate concentrations. This model was based on using partitioning coefficients (K_D) for P onto ferric oxyhydroxides associated with modern hydrothermal plumes (Feely et al., 1998). However, subsequent work showed that the K_D value for P sorption to ferric oxyhydroxides varies

inversely with dissolved silica concentrations, owing to competitive sorption of aqueous silica (Konhauser et al., 2007), and is strongly affected by other components in seawater (e.g., Ca/Mg ratios; Jones et al., 2015). Therefore, there are large uncertainties associated with estimating paleo-phosphate concentrations from P/Fe ratios, and this proxy is likely best suited to delineation of strong, first-order variation, such as that associated with a potential post-Snowball Earth phosphate surplus (Planavsky et al., 2010). Furthermore, the mid-Proterozoic deep-water iron oxide record is exceedingly sparse and is limited to essentially one deposit—the 1.7 Ga Jerome deposit. There is a fairly large range of P/Fe ratios recorded in the Jerome (Planavsky et al., 2010), including values—allowing for uncertainties in partitioning coefficients—indicative of phosphate-limited conditions, as well as those indicative of near-modern phosphate levels.

Although phosphorus undoubtedly played a strong role in controlling rates of primary production in the Proterozoic oceans, the availability of nitrogen, due to trace metal co-limitation (e.g., limitation of nitrogen-fixing activity) or extensive loss of fixed nitrogen under low oxygen conditions, may, on geologically meaningful timescales, have controlled primary productivity over vast stretches of the Precambrian oceans (Anbar and Knoll, 2002; Fennel et al., 2005). Widespread anoxic conditions in Proterozoic oceans would have favored extensive denitrification and anaerobic ammonium oxidation, processes that result in loss of bioavailable nitrogen from the marine system (Fennel et al., 2005). Unfortunately, there are no widely utilized proxies that can directly track the amount of bioavailable N in Proterozoic deep-water settings. However, Mo inventories were likely low in the Proterozoic ocean, given the greater extent of euxinic conditions—relative to the Phanerozoic—under which Mo will be efficiently buried. As Mo is a key micronutrient involved in biological nitrogen fixation, persistent Mo limitation would have resulted in a standing marine N reservoir dramatically less than that of the modern oceans. Therefore, by tracking marine Mo availability, it is possible to find indirect evidence for a small marine N reservoir. There has been a significant amount of work over the last decade focused on tracking the evolution of the marine Mo cycle and its relationship to evolving biospheric redox (see above). The magnitude of Mo enrichments in euxinic shales can, in turn, be used to estimate dissolved marine Mo concentrations. Importantly, the record of Mo enrichments in euxinic marine shales is indicative of bio-limiting dissolved marine Mo concentrations (between 1 and 10 nM compared to >100 nM in the modern ocean; Reinhard et al., 2013a).

PROTEROZOIC CLIMATE AND TECTONICS

Snowball Earth: the most severe climatic perturbation in Earth's history

The most dramatic climatic event of the late Proterozoic is the series of severe Cryogenian glacial episodes, aptly named the 'Snowball Earth' events (Hoffman et al., 1998). The Cryogenian glacials consist of two main phases: the Sturtian glaciation (ca. 717–660 Ma) and the Marinoan glaciation (ca. 640–635 Ma), followed by the less severe and likely more spatially restricted Ediacaran Gaskiers glaciation (ca. 580 Ma) (Fig. 1; Bowring et al., 2003; Rooney et al., 2015). The 'Snowball' Sturtian and Marinoan glaciations are associated with paleomagnetic, sedimentological, stratigraphic, and geochemical evidence indicative of low-latitude and globally widespread, synchronous glaciation (Kirschvink, 1992; Hoffman et al., 1998). This distribution of ice marks a climate state unprecedented in Earth history, with the possible exception of the ca. 2.4–2.2 Ga Huronian glaciations, which were also characterized by low-latitude ice coverage (Fig. 1; Evans et al., 1997). Moreover, the Cryogenian ice ages mark an abrupt end to a nearly 1.5 billion-year ice-free world and the first appearance of Phanerozoic-style icehouse-hothouse cyclicity. Many questions remain concerning the climatic stability of the 1.5 billion years preceding the Cryogenian glacials, and, most importantly, the mechanisms responsible for the shift from a non-glacial to a pan-glacial Earth system remain unresolved. Many have pointed toward a tectonic driver, citing the close timing of the break-up of Rodinia to the initiation of the Cryogenian ice ages (e.g., Halverson et al., 2007; Li et al., 2013; Horton 2015). Given that the Cryogenian glaciations appear uniquely severe relative to other climatic fluctuations in Earth history, this implies that Rodinian breakup paleogeography should have been markedly different from previous and subsequent supercontinent cycles. That may be true for the Phanerozoic supercontinents (Kirschvink, 1992; Evans, 2003).

However, the latest reconstructions of Rodinia's predecessor, Nuna, depict that supercontinent breaking up at similarly low latitudes around 1.3–1.2 billion years ago, during an era completely lacking in glacial deposits. Tectonic driving of long-term paleoclimate may therefore be less important than previously supposed.

A 1.5 billion-year hothouse?

A remarkable span of mid-Proterozoic time, about 1.5 billion years, contains little to no evidence of glaciation on Earth, despite a preponderance of well-preserved sedimentary successions (Evans, 2003). A few notable exceptions have been recognized. Williams (2005) and Kuipers et al. (2013) described what they considered to be sedimentological evidence for glacially mediated erosion and other glacially derived depositional features within basins of well-constrained late Paleoproterozoic age. However, neither study describes sedimentary facies or other features uniquely associated with glacial environments (e.g., dropstones, glacial striations). Geboy et al. (2013) presented a case for a possible late Stenian (ca. 1.2 Ga) glacial diamictite in South America. Using Re-Os geochronology, the authors dated a series of organic-rich shales over- and underlying the glacial diamictite unit within the Vazante Group, constraining the age of the glaciation to between 1.3 and 1.1 Ga (Geboy et al., 2013). This age estimate would place the Vazante Group diamictite well within the Mesoproterozoic. However, these results are in contrast to previous detrital zircon age estimates (<900 Ma) for the glacial deposit (Rodrigues et al., 2012). Given the structural complexity of the region and the importance of such a discovery, the Vazante Group warrants further scrutiny.

Regardless of these putative counterexamples to an otherwise ice-free mid-Proterozoic world, that time interval has fewer glacial deposits than either the preceding (Huronian, 2.4–2.2 Ga) or succeeding (Cryogenian) glacial intervals. However, the presence or lack of evidence for a pan-glacial world does not fully approximate the operation of the Proterozoic climate system. In order to evaluate Proterozoic climate stability more completely, paleoclimatologists face the challenge of developing reliable proxies to measure absolute temperature or establish multiple boundary values to cover a larger range of temperatures. Initial attempts at estimating Proterozoic temperatures made use of $\delta^{18}O$ measurements of sets of chert and phosphate samples from coeval strata. Given that $\delta^{18}O$ of a sedimentary sample is the product of both the precipitant source fluid's initial $\delta^{18}O$ and the temperature-dependent fractionation factor, both can be calculated by using two different minerals sourced from the same fluid but characterized by different fractionation factors. These initial attempts produced surprisingly warm estimates for seawater temperature of ~40°C or higher (Karhu and Epstein, 1986). Such intriguing results appear to be bolstered by both silicon isotopes from Precambrian cherts (Robert and Chaussidon, 2006) and sedimentological observations of the relative rarity of current ripples in Neoarchean turbiditic strata, perhaps an indicator of less viscous seawater at higher temperatures (Fralick and Carter, 2011). However, the silicon-oxygen isotope method has a number of potential pitfalls, chief among them being the multiple origins of chert, between which it is commonly difficult to differentiate (e.g., sedimentary, hydrothermal, volcanic), as well as the potential for metamorphic alteration (see Marin-Carbonne et al., 2014, for a full review). More refined paleotemperature proxies for mid-Proterozoic strata are needed to test these high preliminary paleotemperature estimates—preferably, proxies that will provide a continuous temperature scale rather than a binary signal such as presence or absence of glacial deposits. Only then can climates be distinguished that may have been truly hot versus merely warm, or between temperatures that were temporally stable versus fluctuating significantly above the freezing line.

The Proterozoic atmosphere

Earth's climate over geologic time is dictated by the feedbacks that control the atmosphere's capacity to insulate Earth's surface as well as the surface albedo. This is because Earth's surface temperature is governed by the radiative energy balance: solar radiation is delivered to Earth's surface, and some fraction of this initial radiative flux is reflected away by surface albedo. Because more energy is reflected off Earth's surface than absorbed directly from incoming sunlight, gases in the atmosphere must intercept some of the reflected short-wavelength energy and reflect it back to the surface in order to maintain ambient temperatures (Berner, 1991; Ridgwell and Zeebe, 2005). Understanding ancient climate sensitivity is dependent on recognition of climate-stabilizing feedbacks that modulate Earth's greenhouse effect. During the Archean, the incoming solar

radiation may have been ~30% weaker than today and ~5% weaker during the late Proterozoic ('faint young sun paradox'; Gough, 1981). Thus, a substantially enhanced greenhouse effect would have been required to sustain a hothouse state during Earth's early history.

Although a multitude of gases act as radiation-trapping greenhouse gases (see Byrne and Goldblatt, 2014a for a review), the majority occur in only trace quantities in the atmosphere and play a relatively minor role in determining the overall greenhouse effect. Carbon dioxide (CO_2) plays a major part in modulating recent climate fluctuations; however, it has been argued that methane (CH_4) may have been a dominant greenhouse gas in the Archean (see below; Pavlov et al., 2000, 2003). It has also been hypothesized that NO_x may have potentially functioned as a greenhouse gas, but large fluxes of NO_x to the atmosphere necessitate a euxinic ocean (Buick, 2007), a model that has since fallen out of favor for much of Proterozoic Earth history (Lyons et al., 2014).

Methane is regarded as the major greenhouse gas prior to the Great Oxidation Event. Abundant atmospheric H_2 and low marine sulfate should have resulted in fairly high concentrations of atmospheric methane. In addition, low O_2 concentrations (and thus low oxidative potential) would have increased the residence time of atmospheric methane by a factor of 10^4–10^5 relative to that of today (Kasting, 2005, references therein). However, whether or not methane would have been present as a major atmospheric insulator later in the Proterozoic is highly dependent on the efficiency of methane oxidation, the precise concentration of atmospheric oxygen, and the production rates of atmospheric methane. Large strides have recently been made in modelling atmospheric compositions using 3-D general circulation models (GCMs) with active heat transport (e.g., Charnay et al., 2013; Wolf and Toon, 2014) rather than the 1-D models employed by earlier efforts (e.g., Pavlov et al., 2000). However, ongoing efforts are still hampered by many unknowns and limited constraints from the geological record. Recently, estimates for the radiative forcing of methane have been revised. Low-wavelength methane absorption spectra have been discovered to be stronger than originally thought, and thus methane may not be as powerful of a greenhouse gas at high concentrations as originally modeled (Byrne and Goldblatt, 2014b). In addition, how greenhouse gases interact at different concentrations may further impact their respective insulating capacity (Wordsworth and Pierrehumbert, 2013). Although many questions remain unresolved, it is likely that methane substantially affected Proterozoic atmospheric dynamics. However, it remains to be resolved whether methane played a primary or secondary role relative to CO_2 and other greenhouse gases as a Proterozoic greenhouse gas.

Paleogeography, the supercontinent cycle and a low-latitude Rodinia

Atmospheric CO_2 concentrations and, more broadly, the global carbon budget are controlled by the balance between carbon inputs from volcanism and metamorphism and outputs through organic matter and carbonate burial (Berner, 2004; Ridgewell and Zeebe, 2005). Rates of volcanic and metamorphic carbon outgassing are difficult to constrain in deep time. However, for the sake of discussion we first make the assumption that they have remained constant (see below). Carbonates form through both inorganic and biologically mediated precipitation, and the ingredients necessary to precipitate carbonates are sourced from both the continents (alkalinity and Ca and Mg) and the atmosphere (CO_2), with rates of supply determined in part by rates of silicate weathering on the continents. Organic matter production is largely limited by nutrient supply, which, on geologic time scales, is also largely dependent on silicate weathering-mediated delivery of phosphorus. Both nutrients and alkalinity are weathered from the continental crust by a dissolution reaction with carbonic acid. Weathering rates are sensitive to many factors. However, both CO_2 concentrations and temperature are important parameters in the operation of stabilizing (negative) feedback mechanisms, which ultimately regulate Earth's surface temperature (see Berner, 2004 for a full review). It is important to note that CO_2 outgassing must remain in balance with silicate weathering rates, thus continental weathering rates should not change over geologic timescale unless mirrored by a change in the CO_2 flux to the atmosphere. That said, changes in weathering efficiency will impact atmospheric CO_2 concentrations and temperature by changing equilibrium conditions.

Central to the question of how tectonics affect Earth's climate system is reconstruction of continental configurations and how they have

evolved. Empirical and theoretical evidence accumulated over two decades of research now indicates that Alfred Wegener's Pangea is only the most recent in a series of supercontinents through time (Evans, 2013; Nance et al., 2014). A combination of paleomagnetic, tectonostratigraphic, and geochronologic data has built a strong case for the existence of both the Neoproterozoic supercontinent Rodinia (ca. 900–700 Ma) and the Mesoproterozoic supercontinent Nuna (ca. 1.6–1.3 Ga; alternatively known as Columbia or Hudsonland) (Fig. 6). Recent work has also established the broad outlines of an even older Paleoproterozoic supercontinent, or perhaps a collection of 'supercratons,' referred to as Vaalbara, Superia, and Sclavia (reviewed by Evans, 2013). Supercontinents are described as landmasses where over ~75% of Earth's continental crust forms a single block (Meert, 2012); given their thermal insulation of the upper mantle and influence on mantle convection cells, they are temporally unstable (Gurnis, 1988; Evans, 2003; Li and Zhong, 2009). Tenures of supercontinents are suspected to mark inflection points for changes in tectonic and paleoenvironmental parameters (e.g., global arc length, large igneous province frequency; Bradley, 2011). As such, Proterozoic supercontinent episodicity has been of great interest to researchers of the broader Earth system. Although the 'boring billion' interval encompasses the amalgamation and breakup of two supercontinents, only Rodinia was followed by dramatic changes in Earth's climate state ('Snowball Earth'), begging the question of what tectonic and climatic factors were unique in paving the way for Cryogenian icehouse conditions.

An interesting feature of the early Neoproterozoic is the concentration of continents near the paleo-equator (Li et al. 2013; Fig. 6). Equatorial regions received much more rainfall, and are characterized by higher temperature and, as a result, higher chemical weathering rates. The break-up of Rodinia would, by fragmenting the continents, have increased the continental surface area proximally exposed to oceanic moisture (Donnadieu et al., 2004). Continental configuration also plays an important role in modulating Earth's effective surface albedo. Although clouds are the most effective reflectors of incoming radiation back into space, continents have a higher albedo than open water, thus, a concentration of landmasses near the equator should result in a higher effective albedo (Endal and Schatten, 1982). Such a continental configuration could have increased Earth's reliance on greenhouse gases to maintain temperature stability. The low-latitude continental configuration prior to the Cryogenian glaciations has commonly been considered to play a key role in the initiation of glaciation (e.g., Schrag et al., 2002). During initial stages of glaciation, glaciers may have formed in the polar regions without inhibiting chemical weathering and CO_2 drawdown in equatorial regions (Kirschvink, 1992; Hoffman et al., 1998), leading to runaway glacial feedback. However, it is unclear whether paleocontinental configuration differed substantially between Rodinia and its Mesoproterozoic predecessor Nuna, which lacks associated glacial events. A fully developed and tested paleomagnetic/tectonostratigraphic model has yet to emerge; however, enough data are available to confirm the low-latitude position of most cratons at the start of the Cryogenian (Fig. 6; Li et al., 2013). What remains to be determined are better estimates of total land-mass area (including the contemporaneous extent of current microcontinental fragments embedded within younger orogenic collages), the precise paleolatitudes of continent-continent collisions and mountain chains, and tighter paleolongitudinal constraints that could be used in integrated ocean-atmosphere geochemical models similar to those of the Phanerozoic (e.g., Golonka and Krobicki, 2012). Recent tectonostratigraphic and paleomagnetic work has begun to piece together the history of Nuna, including its location, latitudinal distribution, and size (e.g., Evans and Mitchell, 2011; Pisarevsky et al., 2014; Pehrsson et al., 2015), but paleogeographic details remain a distant target. The models broadly place Nuna, like Rodinia, at low latitudes, especially at the time of breakup (Fig. 6).

The emplacement of large igneous provinces (LIP) has occurred at variable rates over geologic time (Fig. 7), with troughs during supercontinent assembly and peaks during supercontinent break-up (Ernst et al., 2008). Each LIP volcanic event is typically of such short duration that it may contribute little to the long-term atmospheric carbon pool. However, because basalts have the potential to weather much more rapidly than felsic materials (Dessert et al., 2003), the concurrence of a peak in LIP volcanism with the breakup of Rodinia (Fig. 6) has been cited as a possible trigger for the Cryogenian glaciations, due to

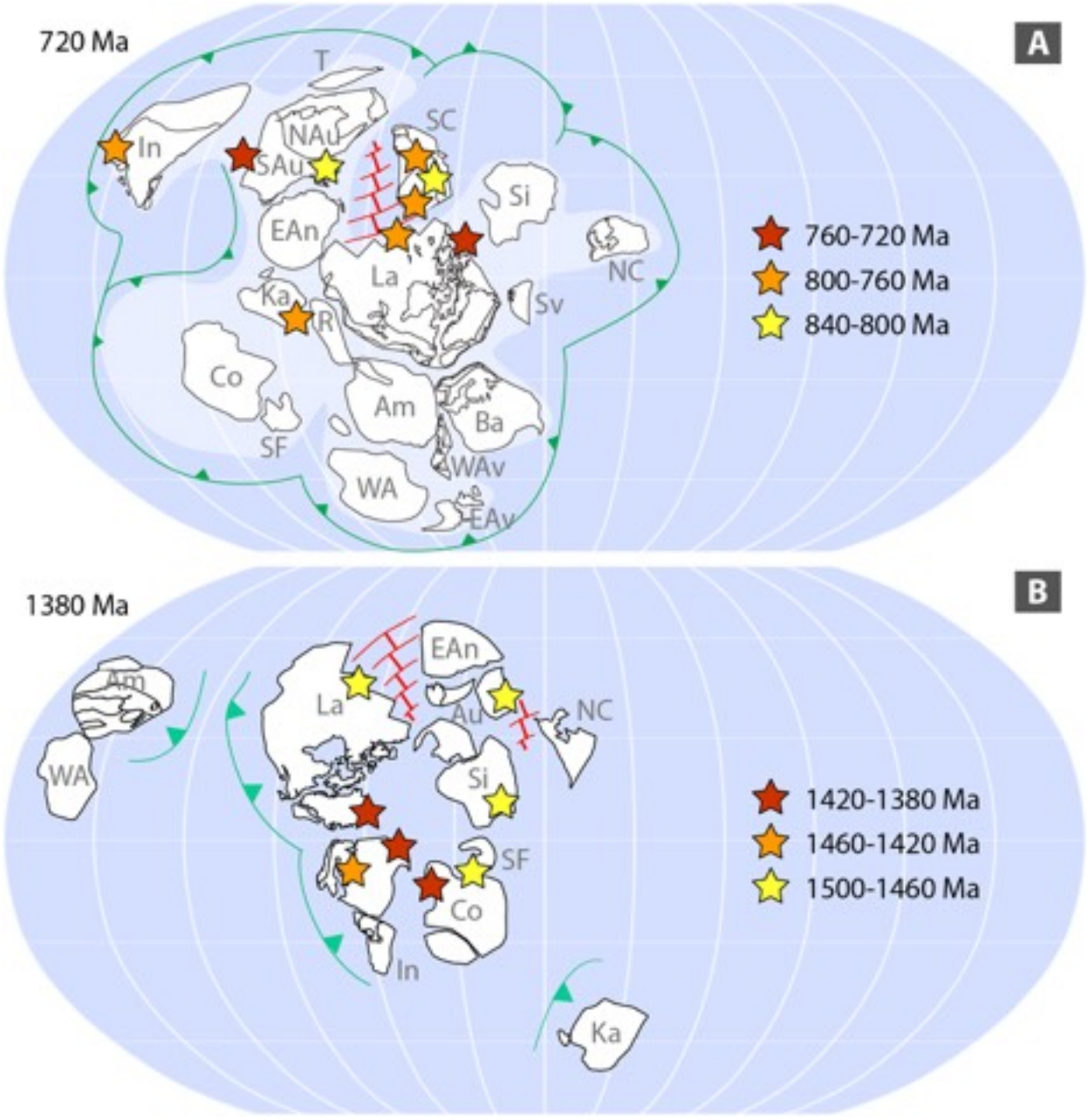

FIGURE *6*.—Comparison of the breakup paleogeographies of Proterozoic supercontinents. A) Rodinia, modified from Li et al. (2013). B) Nuna, using rotation parameters from Pisarevsky et al. (2014). Stars indicate presumed plume centers from the compilation in Ernst (2015). Craton abbreviations: Am=Amazon, Au=(proto)Australia, Ba=Baltica, Co=Congo, EAn=East Antarctica, EAv=East Avalonia, In=India, Ka=Kalahari, La=Laurentia, NAu=northern Australia, NC=North China, R=Rio Plata, SAu=southern Australia, SC=South China, SF=São Francisco, Si=Siberia, T=Tarim, WA=West Africa, Wav=West Avalonia. In the oceanic realm, green curves are subduction systems (barbs on upper plate), and red lines delineate seafloor spreading systems.

atmospheric CO_2 drawdown concomitant with silicate weathering (Godderis et al., 2003; Donnadieu et al., 2004). In addition to fostering rapid weathering, LIPs are enriched in P relative to average continental crust; thus, an increase in LIP weathering could potentially drive a large increase in P delivery to the ocean, stimulating organic matter production and drawing down CO_2 (Horton, 2015). However, few LIPs remain exposed at the surface, as hundreds of millions of years of erosion have left us with little more than dike swarms as evidence for Proterozoic LIPs.

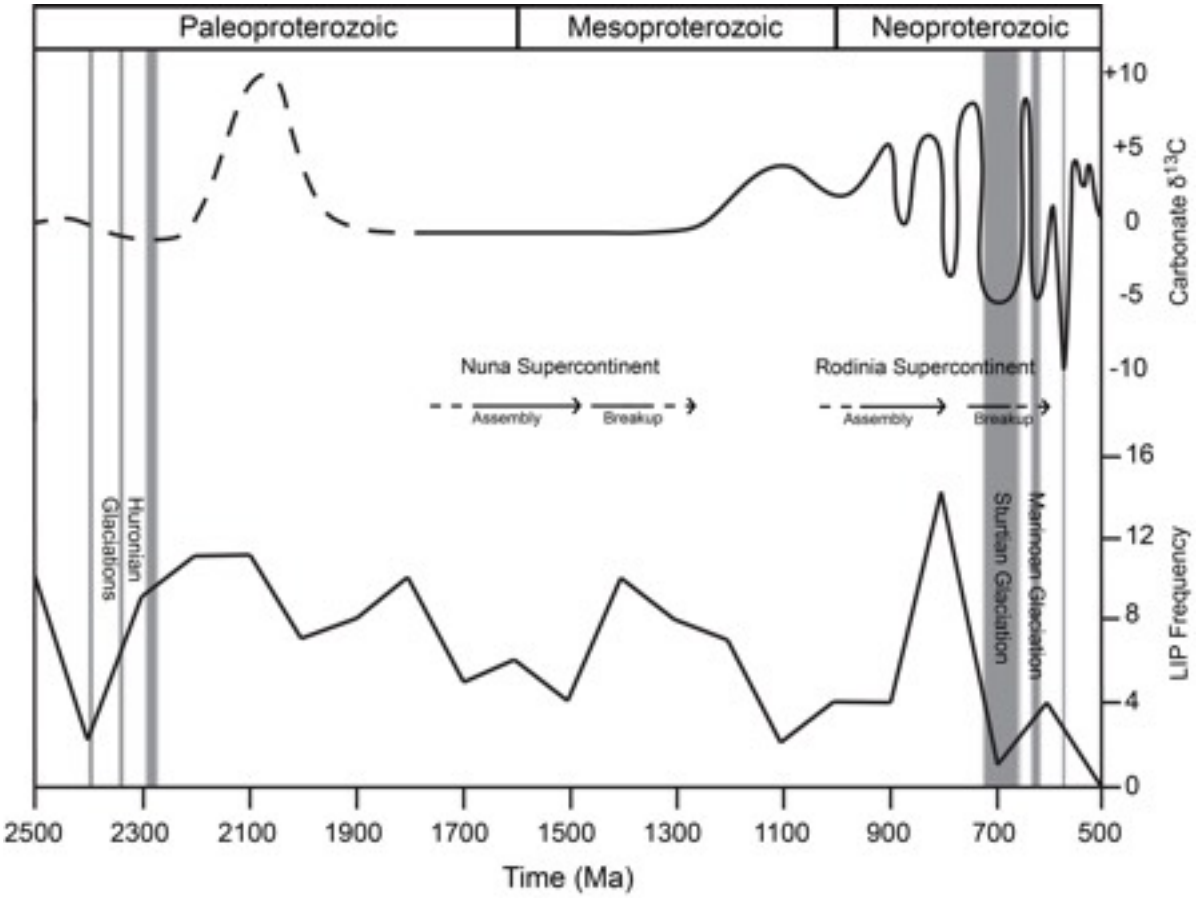

FIGURE 7.—Joint records of emplacement of Large Igneous Provinces (LIPs), carbonate $\delta^{13}C$, and supercontinent assembly and breakup. Peak frequency of LIP emplacement appears to coincide with the initial stages of supercontinent breakup. Frequency of LIPs tabulated in named events per 100 million-year interval. Solid and dashed lines of $\delta^{13}C$ curve denote relative degree of resolution of these data. Data from Ernst et al. (2013), Halverson et al. (2010), and Kah et al. (1999).

Therefore, estimating areal extent, LIP thickness, and thus the volume of basalt, is a difficult task (Bryan and Ernst, 2008; Ernst et al., 2008), and calculation of the impact of LIPs on marine alkalinity and CO_2 drawdown remains a considerable challenge. Assuming that these challenges are shared for all Precambrian LIPs, their relative abundance during times of supercontinental breakup remains a valid first-order observation (Fig. 7; Ernst et al., 2013) and should imply similar tectonic forcing to the surface paleoenvironment, given that continental latitudes were broadly similar at ca. 1300 and 800 Ma (Fig. 6). Overall, the gross similarity of Nuna and Rodinia paleogeographies, including emplacement of LIPs, at their times of fragmentation begs the question of why ensuing paleoclimates should have differed so fundamentally: i.e., late Mesoproterozoic hothouse versus early Cryogenian Snowball Earth. Could global tectonics be more like a passenger than a driver of long-term paleoclimatic patterns?

Continental arc magmatism

The majority of work exploring the role played by tectonics as a paleoclimate driver, (and thus much of the above discussion) has focused on how carbon is sequestered from the atmosphere (e.g., Edmond, 1992; Berner, 2001). However, changes in carbon outgassing may produce just as large, if not larger, changes in climate (Lee et al., 2015). Due to the challenges of directly measuring carbon degassing from volcanism and metamorphism, most estimates of outgassing have traditionally been calculated by means of a mass-balance approach (e.g., Berner, 1991). Recently, however, there has been a push to identify the relative importance of different outgassing fluxes and how they may have varied over geologic

time.

Outgassing of mantle and crustal carbon has three chief sources: 1) metamorphic decarbonation of sediments, 2) outgassing of mid-ocean ridge basalts, and 3) decarbonation of subducted crust and continental sediments during arc magmatism (Dasgupta, 2013; Lee et al., 2013). The high-CO_2 record of the Cretaceous provides an excellent natural laboratory to examine these interactions in greater detail. Lee et al. (2013) noted that high CO_2 concentrations during the Cretaceous could be a byproduct of increased CO_2 outgassing. The authors pointed toward continental arc complexes as a possible culprit, and proposed that a 2–2.8-fold increase in CO_2 outgassing could account for the 'excess' atmospheric carbon indicated by Cretaceous pCO_2 proxies. The authors linked this excessive CO_2 outgassing to the abundance of continental arc complexes. Of particular importance is the Cretaceous shift from island arc-dominated subduction zones (as are common today) to continental arc-dominated subduction zones (Lee et al., 2013; Ducea et al., 2015). The significance of this shift hinges upon the disparate composition of continental and volcanic crust—rising magma in a continental arc system must penetrate continental crust, which is relatively rich in sedimentary carbonates. Due to the high temperatures associated with arc magmatism, sediments are metasomatically incorporated into rising magma, and carbonate minerals are efficiently decarbonated to release CO_2 (Lee et al., 2013). As such, the greater length of volcanic arcs and higher relative abundance of continental arcs during the Cretaceous would have considerably influenced the magnitude of CO_2 outgassing. Due to the high temperatures associated with arc-magmatism, sediments are metasomatically incorporated into rising magma, and carbonate minerals are efficiently decarbonated to release CO_2 (Lee et al., 2013). As such, the greater length of volcanic arcs and higher relative abundance of continental arcs during the Cretaceous would have considerably influenced the magnitude of contemporaneous CO_2 outgassing. In addition to mediating increased CO_2 output, continental arcs are also significant contributors to global topographic highs, driving topographic uplift of thin narrow mountain ranges, which are conducive to more intensive weathering and thus CO_2 consumption (Lee et al., 2015). Uplift-mediated high rates of CO_2 consumption may, during the lifetime of these continental arcs, have been outweighed by the excessive CO_2 flux associated with increased volcanism. However, once subduction halts and magmatism is reduced, this combination of decreased CO_2 outgassing and continual weathering of topographic highs will result in net CO_2 consumption, inducing a strong cooling effect (Lee et al., 2015).

How this model fits into a supercontinent framework and can be applied to the deep past has yet to be explored in great detail. In a similar fashion to LIPs, continental arc length should be dependent on the supercontinent cycle, as continent-continent collisions must be preceded by continental arc subduction. Periods of supercontinent amalgamation will be associated with peaks in the abundance and activity of continental arcs, whereas periods of continental breakup should be associated with decreased continental arc subduction. McKenzie et al. (2014) proposed that detrital zircon datasets could be used to estimate continental arc length in the geologic past. Zircons are a common trace mineral in intermediate to felsic igneous rocks and are highly resistant to mechanical and chemical weathering. Continental arc settings are particularly efficient at preserving recently erupted zircons (Cawood et al., 2012). Using samples with independent age constraints, McKenzie et al. (2014) reasoned that time periods characterized by a high concentration of continental arcs should show detrital zircon age peaks in close proximity to the true depositional age of the sample from which they were measured. On the other hand, intervals characterized by low continental arc activity should possess more broadly distributed detrital zircon ages. Detrital zircon age compilations across the Neoproterozoic show that the Cryogenian was characterized by reduced continental arc activity (McKenzie et al., 2014). It follows from this relationship that the early Cryogenian may have been characterized by reduced CO_2 concentrations, which in turn may have contributed to the initiation of the Cryogenian ice ages.

Careful consideration of the cumulative effect of changes in continental arc length and continental weathering feedbacks has led to more refined estimates of the impact of tectonics on Earth's climate through time. However, a number of outstanding questions remain. Carbon outgassing, as discussed above, is not confined to arc magmatism alone. To continue using the

example of the Cretaceous by Lee et al. (2013), degassing from mid-ocean ridge basalts scales linearly with spreading rate and ridge length. Rowley (2002) has suggested that oceanic crust production rates over the past 200 million years have remained constant within 20%; however, Müller et al. (2008) and Becker et al. (2008) (among others) argued for much faster spreading rates in the Cretaceous. Thus, mid-ocean ridge spreading may also be a major source of heightened CO_2 during the Cretaceous. Furthermore, lingering uncertainties remain concerning the relative carbon flux of each source as well as the extent to which carbon degassing from continental arcs is sourced from sedimentary metasomatism rather than subducted sediments (Kelemen and Manning, 2015). While the difference between subducted seafloor sediments and continental crust-derived sediments may appear a subtle distinction, deep marine carbonates are a relatively recent occurrence in Earth history, dating back to only the mid-Mesozoic, and their emergence in the geologic record would have profoundly influenced the arc magmatism-associated carbon budget. Extension of the approach of McKenzie et al. (2014) to the Mesoproterozoic may reveal whether similar tectonic drivers may have been at work in the interval spanning the breakup of Nuna, which could shed further light on why the disassembly of Rodinia and Nuna were characterized by fundamentally disparate climatic conditions.

THE IMPACT OF EUKARYOTIC EVOLUTION ON CARBON CYCLING AND EXPORT PRODUCTIVITY

The evolution of eukaryotes, and particularly the transition of the oceans from Precambrian-style prokaryote-dominated primary production to Phanerozoic-style eukaryote-dominated primary production would have had a profound impact upon Earth's carbon cycle, and thus on climate dynamics and oxygen levels. It is commonly proposed that the rise of eukaryotes may have had a more dramatic impact than tectonic drivers did upon the carbon cycle. It has been suggested that the replacement of cyanobacteria by eukaryotes as the predominant phytoplankton of the global ocean, as well as the emergence of metazoan zooplankton, would, by virtue of greater cell size and fecal pellet repackaging of organic matter, have increased rates of particulate organic carbon (POC) settling. Higher rates of export delivery, in turn, have been proposed to have enhanced water-column clarity and thus the colonization of the shallow-ocean benthos by eukaryotic macrophytes, leading to the development of complex benthic ecosystems, as well as decreased water-column respiration and higher rates of organic carbon burial (Logan et al., 1995; Butterfield, 2011).

Metazoan zooplankton undoubtedly strongly influence surface-ocean and export productivity in the modern ocean. The presence of heterotrophic zooplankton likely played a major role in the emergence of large and biomineralized phytoplankton (e.g., Butterfield, 2011), and the repackaging of surface ocean-produced organic carbon into zooplankton (particularly macrozooplankton) and fish fecal pellets strongly influences the modern medium and delivery of POC (Turner, 2002). In contrast, coprophagous zooplankton (particularly micro- and mesozooplankton) also disaggregate fecal pellets, thereby reducing POC settling and benthic delivery rates (Dilling and Alldredge, 2000; Iversen and Poulsen, 2007). The net effect of metazoans on the biological pump, even in the modern oceans, is not straightforward (Turner, 2002). Regardless, metazoan zooplankton do not appear unambiguously in the fossil record until the Phanerozoic and are therefore unlikely to have played an immediate role in engineering the earliest stages of the transformation of the oceans to a eukaryote-dominated system.

Importantly, even in the modern ocean, particle aggregation and sinking are not controlled by zooplankton-mediated fecal packaging and disaggregation alone; a number of other processes strongly influence export productivity. Nor is size, as has been previously suggested (e.g., Butterfield, 2011), necessarily the most important factor in determining rate of POC settling. For instance, density, porosity, and composition may play an equal or even greater role in the sinking rates of both particles and marine snow aggregates (Ploug et al., 2008).

Through ballasting, detrital and biogenic minerals, such as lithogenic dust, diatomaceous opal, and coccolithophore-derived carbonate, appear to play a particularly strong role in POC aggregation and settling and may even constitute half the mass of settling particles (Armstrong et al., 2002; Klaas and Archer, 2002; Ploug et al., 2008; Fischer and Karakaş, 2009; Fischer et al., 2009). Empirical and experimental observations suggest that coccolithophoran calcium carbonate

and lithogenic dust play a stronger role than diatomaceous opal in POC ballasting (Klaas and Archer, 2002; Fischer and Karakaş, 2009; Fischer et al., 2009); organic particles rich in carbonate biominerals and dust are commonly characterized by higher densities and settling velocities (Ploug et al., 2008). In the vicinity of arid continental regions, such as along the northwest African coast, the correlation of lithogenic dust contents and POC settling rates is pronounced (Fischer et al., 2009). During the Tonian, concurrent with the development of eukaryotic production (and hundreds of millions of years prior to the emergence of coccolithophores and diatoms), dust would have played a much greater role, proportionally, in POC ballasting. The impact of dust on both surface-ocean and export productivity may have been further enhanced by the onset of Cryogenian glacial conditions, which, as observed for Cenozoic glacials (Petit et al., 1999; Klaas and Archer, 2002), may have been associated with heightened aridity, a reduced hydrological cycle, and thus increased delivery of dust to the oceans. This might be one factor that allowed for continued carbon dioxide drawdown during ice advance. Therefore, in spite of the lack of zooplankton fecal packaging, early eukaryote-dominated and even prokaryote-dominated planktonic communities were likely associated with high export productivity.

NUTRIENT CYCLES, THE CARBON CYCLE, AND REDOX EVOLUTION

There is strong evidence for the persistence of a largely anoxic ocean through the mid-Proterozoic. Furthermore, there is strong potential for very low (<<1% PAL) atmospheric oxygen levels over the same interval. Given that organic carbon remineralization is inhibited under anoxic conditions (Kastev and Crowe, 2015), it is likely that nutrient limitation is necessary to maintain low surface oxygen levels for extended periods of time. Therefore, there is an obvious impetus to explore the mechanisms by which reducing oceans may have induced severe nutrient limitation.

It is clear that marine nutrient cycles shifted with the protracted oxygenation of Earth's surface. In an ocean characterized by widespread iron-rich conditions, it was likely possible to trap P in deeper portions of the ocean through scavenging and downward transport on Fe oxides, potentially limiting the supply of P available for upwelling in large regions of the ocean and introducing pronounced P stress to photic-zone ecosystems. A deep-sea P trap (P burial with oxides or as vivianite) is likely to have lowered the size of the marine P reservoir and to have thus decreased net marine productivity.

Moreover, in an anoxic ocean, large amounts of bioavailable N can be lost from the marine system through denitrification and anaerobic ammonium oxidation (anammox) (Kuypers et al., 2003). Extensive loss of bioavailable N in an ocean characterized by oxic surface waters and anoxic deep waters likely would have led to N stress. Additionally, inventories of the trace metal Mo, which is an essential component in enzymatic nitrogen fixation, were also likely smaller in the Proterozoic ocean, given the occurrence of more widespread euxinic conditions. There is compelling evidence that Proterozoic deep oceans were rich in dissolved iron, rather than euxinic, as was once commonly thought. However, as stressed above, euxinia in the mid-Proterozoic ocean was likely orders of magnitude more widespread than in the modern ocean, and even a relatively small areal extent of euxinic seafloor might have been sufficient to favor drawdown of the Mo reservoir. In this light, the distinction should be made between a geochemically sulfidic ocean (deep-ocean euxinia) and a biologically sulfidic ocean (where trace nutrient limitation of marine primary producers is strongly controlled by the spatial extent of euxinic conditions.

In sum, a strong case can be made for dramatically lower marine N and P levels over long intervals of the Proterozoic relative to the Phanerozoic, and that nutrient stress was likely tied to marine redox conditions. The driving question then centers on the factors that allowed the Earth system to move out of this state. There are several potentially linked drivers. Tectonic factors may have pushed the Earth system out of this oxygen-limited 'stasis.' For instance, accumulation of continents in the rain belts and/or extensive basaltic emplacement may have resulted in intense weathering and increased P release (Horton, 2015; see above). Alternatively, a biological trigger may have been responsible for this transition. For instance, it is possible that the diversification of eukaryotes increased organic carbon burial (e.g., Butterfield, 2011; see above). As stressed above, however, the larger size of eukaryotic phytoplankton relative to prokaryote producers does not necessarily lead to more

efficient carbon export, and thus the transformation of planktonic communities to eukaryote-dominated systems would not necessarily have led to dramatic increases in carbon export and burial. Ultimately, despite recent advances, what is needed to resolve the feasibility of various models for Proterozoic oxygenation are better constraints on marine nutrient levels and a more finely temporally resolved record of redox and biological diversification.

THE ROLE OF ENVIRONMENTAL OXYGEN LEVELS IN EARLY METAZOAN EVOLUTION

It has long been hypothesized that secular changes in the amount of molecular oxygen (O_2) in Earth's oceans and atmosphere have played a significant role in the evolution of early animal life (e.g., Nursall, 1959). This is an intuitively appealing notion, given the energetic payoff of using O_2 as a respiratory oxidant (Lane and Martin, 2010), its importance in the basic biochemistry of eukaryotic life (Towe, 1970; Summons et al., 2006), and its role through ozone formation in maintaining a clement Earth surface shielded from the harmful effects of solar ultraviolet radiation. As a result, a large body of work has sought to bridge reconstructed environmental oxygen levels prior to and during the period of metazoan emergence with characterizations of the O_2 levels required for animal life to emerge and proliferate (e.g., Runnegar, 1991; Canfield et al., 2007; Mills et al., 2014; Planavsky et al., 2014).

Much of this discussion has been framed in terms of 'threshold' O_2 levels required for basal eukaryotic or metazoan taxa, where efforts to theoretically (Runnegar, 1991; Sperling et al., 2013) or empirically (Mills et al., 2014) estimate the O_2 levels needed for a discrete life stage of a given representative basal metazoan are compared to geochemical reconstructions of ambient environmental oxygen levels (e.g., Canfield et al., 2007; Planavsky et al., 2014). Within this context, recent empirical estimates of ocean-atmosphere oxygen levels suggesting an upper background level of less than ~0.1% of PAL for large portions of the mid-Proterozoic (Planavsky et al., 2014) imply that early metazoan life might have faced severe metabolic challenges and perhaps large surface UV fluxes (Fig. 8). However, it is important to note that it is possible that numerous substrates, including water, can lead to rapid UV

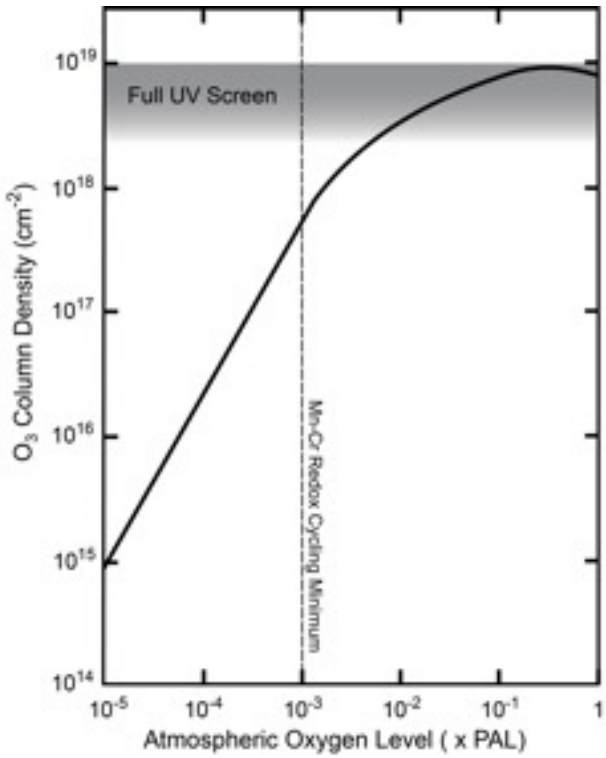

FIGURE 8.—Column depth of ozone as a function of ground-level atmospheric oxygen concentrations. Shaded box indicates the column depths required for significant absorption of biologically harmful ultraviolet radiation. Also shown is the estimated upper limit in atmospheric pO_2 inferred from coupled Mn-Cr cycling (e.g. Planavsky et al., 2014). After Catling (2014).

attenuation. Furthermore, the concentration of atmospheric methane and the presence or absence of atmospheric organic haze, and atmospheric S chemistry (Kasting et al., 1989) and Cl chemistry (Singh and Kasting, 1988) may also affect atmospheric ozone chemistry and the extent of UV shielding.

However, current understanding of the relationship between environmental O_2 levels and early animal evolution suffers from a number of deficiencies. First, quantitatively estimating O_2 levels in deep time is an exceptionally difficult problem, one that requires greater precision from existing and emerging geochemical proxies. Second, surface ocean environments have likely been diverse throughout Earth's history on spatial and temporal scales that differed from the first-order, longer-term 'background' patterns often inferred from geochemical proxies. Third, the 'threshold' concept for O_2 limitation of basal metazoan organisms does not explicitly incorporate a consideration of variable oxygen

demand during different stages of an organism's life history. Finally, a sharp focus on O_2 may obscure the likely important role of synergistic physiological effects involving the combined impacts of O_2 and other key environmental variables, such as pCO_2 or temperature. Addressing these issues will require more refined quantitative models for inverting O_2 from geochemical data, empirical data sets that account for spatiotemporal variability, and biological/ecological models that incorporate the complexities of physiological synergism, life history, and spatial ecology.

CONCLUSIONS

Earth's middle age, the mid-Proterozoic, ca. 1.8 to 0.8 billion years ago, was defined by an array of redox and nutrient feedbacks that maintained a remarkable stability in the carbon cycle and suppressed the radiation of eukaryotic organisms and ocean-atmosphere oxygenation for over a billion years. How and when this cycle was broken and the Earth moved beyond the 'boring billion,' in phase with extreme glaciations, increased oxygenation, and ultimately the emergence of animals, remain among the crucial questions in the history of Earth-life co-evolution. Previous work points to a mid-Proterozoic marked by very low ocean-atmosphere oxygen availability and concomitant nutrient limitations that challenged the diversity and abundance of early eukaryotic life. In contrast, there is evidence for rising oxygen during the latest Proterozoic and the parallel rise of animal life. Despite these advances, a debate still lingers about the relative roles of intrinsic and extrinsic drivers in the diversification of eukaryotes and the appearance and early evolution of animals, including cause-and-effect relationships with oxygen and climatic extremes. Resolution can only be found by looking back at the trajectories leading from the remarkable stasis of the mid-Proterozoic to the dramatic change of the late Neoproterozoic; this Earth-life transition is where much current research interest lies.

ACKNOWLEDGMENTS

N.J.P., T.W.L., G.D.L., and C.T.R were supported by the NSF-ELT program. L.G.T.'s research was supported by a Yale University Postdoctoral Associateship and the Foundations of Complex NASA Astrobiology Institute. D.A.D. was supported by the Alternative Earth's NASA Astrobiology Institute. We are grateful to Nathan Sheldon for feedback on the manuscript.

REFERENCES

Anbar, A. D., Y. Duan, T. W. Lyons, G. L. Arnold, B. Kendall, R. A. Creaser, A. J. Kaufman, G. W. Gordon, C. Scott, J. Garvin, and R. Buick. 2007. A whiff of oxygen before the Great Oxidation Event? Science, 317:1903–1906.

Anbar, A. D., and A. H. Knoll. 2002. Proterozoic ocean chemistry and evolution: A bioinorganic bridge? Science, 297:1137–1142.

Anderson, R. P., F. A. Macdonald, N. J. Tosca, T. Bosak, U. Bold, and D. E. G. Briggs. 2014. Taphonomy of eukaryotic microfossils between Cryogenian ice ages explored in the Zavkhan Terrane, southwestern Mongolia [Abstract]. Geological Society of America Abstracts with Programs 46(6):542.

Armstrong, R. A., C. Lee, J. I. Hedges, S. Honjo, and S. G. Wakeham. 2002. A new, mechanistic model for organic carbon fluxes in the ocean based on the quantitative association of POC with ballast minerals. Deep-Sea Research Part II-Topical Studies in Oceanography, 49:219–236.

Arnold, G. L., A. D. Anbar, J. Barling, and T. W. Lyons. 2004. Molybdenum isotope evidence for widespread anoxia in Mid-Proterozoic oceans: Science, 304:87–90.

Auerbach, D., N. Planavsky, N. Alfimova, C. T. Reinhard, X. Wang, and D. Asael. 2014. A terrestrial Mesoarchean–Mesoproterozoic record of atmospheric oxygen levels [Abstract]. Geological Society of America Abstracts with Programs, 46(6):520.

Bailey, T., J. Mcarthur, H. Prince, and M. Thirlwall. 2000. Dissolution methods for strontium isotope stratigraphy: whole rock analysis. Chemical Geology, 167:313–319.

Becker, T. W., C. P. Conrad, B. Buffett, and R. D. Müller. 2009. Past and present seafloor age distributions and the temporal evolution of plate tectonic heat transport. Earth and Planetary Science Letters, 278:233–242.

Bekker, A. 2015. Questioning myths of the middle Proterozoic time [Abstract]. AGU-GAC-MAC Joint Assembly, Montreal, Quebec.

Berner, R. A. 1991. A model for atmospheric CO_2 over Phanerozoic time. American Journal of Science, 29:339–376.

Berner, R. A. 2004. The Phanerozoic Carbon Cycle: CO_2 and O_2. Oxford University Press.

Berner, R. A., and Z. Kothavala. 2001. GEOCARB III: A revised model of atmospheric CO_2 over Phanerozoic time. American Journal of Science, 301:182–204.

Bjerrum, C. J., and D. E. Canfield. 2002. Ocean productivity before about 1.9 Gyr ago limited by phosphorus adsorption onto iron oxides. Nature, 417:159–162.

Blumenberg, M., V. Thiel, W. Riegel, L. C. Kah, and J. Reitner. 2012. Biomarkers of black shales formed by microbial mats, Late Mesoproterozoic (1.1 Ga) Taoudeni Basin, Mauritania. Precambrian Research, 196–197:113–127.

Bowring, S. A., P. M. Myrow, E. Landing, J. Ramezani, D. Condon, And K. Hoffmann. 2003. Geochronological constraints on Neoproterozoic glaciations and the rise of metazoans. Geological Society of America Abstracts with Programs, 35(6):516.

Bradley, D.C. 2011. Secular trends in the geologic record and the supercontinent cycle: Earth-Science Reviews,108:16–33.

Brand, U., and J. Veizer. 1980. Chemical diagenesis of a multicomponent carbonate system; 1, Trace elements. Journal of Sedimentary Research, 50:1219–1236.

Brand, U., G. Jiang, K. Azmy, J. Bishop, and I. P. Montañez. 2012. Diagenetic evaluation of a Pennsylvanian carbonate succession (Bird Spring Formation, Arrow Canyon, Nevada, U.S.A.)—1: Brachiopod and whole rock comparison. Chemical Geology, 308–309:26–39.

Brocks, J. J., G. D. Love, R. E. Summons, A. H. Knoll, G. A. Logan, and S. A. Bowden. 2005. Biomarker evidence for green and purple sulphur bacteria in a stratified Palaeoproterozoic sea. Nature, 437:866–870.

Brocks, J. J., and A. Pearson. 2005. Building the biomarker tree of life. Molecular Geomicrobiology, 59:233–258.

Bryan, S. E., and R. E. Ernst. 2008. Revised definition of Large Igneous Provinces (LIPs). Earth-Science Reviews, 86:175–202.

Buick, R. 2007. Did the Proterozoic 'Canfield Ocean' cause a laughing gas greenhouse? Geobiology, 5:97–100.

Butterfield, N. J. 2000. *Bangiomorpha pubescens* n. gen., n. sp.: implications for the evolution of sex, multicellularity, and the Mesoproterozoic/ Neoproterozoic radiation of eukaryotes. Paleobiology, 26:386–404.

Butterfield, N. J. 2011. Animals and the invention of the Phanerozoic Earth system. Trends in Ecology & Evolution, 26:81–87.

Byrne, B., and C. Goldblatt. 2014a. Radiative forcings for 28 potential Archean greenhouse gases. Climate of the Past Discussions, 10:2011–2053.

Byrne, B., and C. Goldblatt. 2014b. Radiative forcing at high concentrations of well-mixed greenhouse gases. Geophysical Research Letters, 41:152–160.

Canfield, D. E. 1998. A new model for Proterozoic ocean chemistry. Nature, 396:450–453.

Canfield, D. E. 2005. The early history of atmospheric oxygen: Homage to Robert M. Garrels: Annual Review of Earth and Planetary Sciences, 33:1–36.

Canfield, D. E., S. W. Poulton, A. H. Knoll, G. M. Narbonne, G. Ross, T. Goldberg, and H. Strauss. 2008. Ferruginous conditions dominated later Neoproterozoic deep-water chemistry. Science, 321:949–952.

Canfield, D. E., S. W. Poulton, and G. M. Narbonne. 2007. Late-Neoproterozoic deep-ocean oxygenation and the rise of animal life. Science, 315:92–95.

Canfield, D. E., and R. Raiswell. 1999. The evolution of the sulfur cycle. American Journal of Science, 299:697–723.

Cavalier-Smith, T. 2002. The neomuran origin of Archaebacteria, the negibacterial root of the universal tree and bacterial megaclassification. International Journal of Systematic and Evolutionary Microbiology, 52:7–76.

Cawood, P. A., C. J. Hawkesworth, and B. Dhuime. 2012. Detrital zircon record and tectonic setting. Geology, 40:875–878.

Charnay, B., F. Forget, R. Wordsworth, J. Leconte, E. Millour, F. Codron, and A. Spiga. 2013. Exploring the faint young Sun problem and the possible climates of the Archean Earth with a 3-D GCM. Journal of Geophysical Research: Atmospheres, 118:10,414–10,431.

Clites, E. C., M. L. Droser, and J. G. Gehling. 2012. The advent of hard-part structural support among the Ediacara biota: Ediacaran harbinger of a Cambrian mode of body construction. Geology, 40:307–310.

Cohen, P. A., and A. H. Knoll. 2012. Scale microfossils from the mid-Neoproterozoic Fifteenmile Group, Yukon Territory. Journal of Paleontology, 86:775–800.

Cole, D., M. Hodgskiss, B. Gueguen, M. Kunzmann, P. Crockford, T. Gibson, S. Worndle, G. Halverson, and N. Planavsky. 2015. Redox conditions in the latest Mesoproterozoic [Abstract]. Goldschmidt Annual Meeting. Prague, Czech Republic.

Dasgupta, R. 2013. Ingassing, storage, and outgassing of terrestrial carbon through geologic time. Reviews in Mineralogy and Geochemistry, 75:183–229.

Derry, L. A. 2010. A burial diagenesis origin for the Ediacaran Shuram–Wonoka carbon isotope anomaly. Earth and Planetary Science Letters, 294(1–2):152–162.

Dessert, C., B. Dupré, J. Gaillardet, L. M. François, and C. J. Allègre. 2003. Basalt weathering laws and the impact of basalt weathering on the global carbon cycle. Chemical Geology, 202(3–4):257–273.

Dilling, L., and A. L. Alldredge. 2000. Fragmentation of marine snow by swimming macrozooplankton:

A new process impacting carbon cycling in the sea. Deep-Sea Research Part I-Oceanographic Research Papers, 47:1227–1245.

Donnadieu, Y., Y. Godderis, G. Ramstein, A. Nedelec, and J. Meert. 2004. A "Snowball Earth" climate triggered by continental break-up through changes in runoff. Nature, 428:303–306.

Douzery, E. J. P., E. A. Snell, E. Bapteste, F. Delsuc, and H. Philippe. 2004. The timing of eukaryotic evolution: Does a relaxed molecular clock reconcile proteins and fossils? Proceedings of the National Academy of Sciences of the United States of America, 101:15386–15391.

Driese, S. G., and L.G Medaris. 2008. Evidence for biological and hydrological controls on the development of a Paleoproterozoic paleoweathering profile in the Baraboo Range, Wisconsin, USA. Journal of Sedimentary Research, 78:443–457.

Driese, S. G., E. L. Simpson, and K. A. Eriksson. 1995. Redoximorphic paleosols in alluvial and lacustrine deposits, 1.8 Ga Lochness Formation, Mount-Isa, Australia—pedogenic processes and implications for paleoclimate. Journal of Sedimentary Research, 65: 675–689.

Droser, M. L., J. G. Gehling, and S. R. Jensen. 2006. Assemblage palaeoecology of the Ediacara biota: The unabridged edition? Palaeogeography Palaeoclimatology Palaeoecology, 232(2–4):131–147.

Ducea, M. N., J. B. Saleeby, and G. Bergantz. 2015. The architecture, chemistry, and evolution of continental magmatic arcs. Annual Review of Earth and Planetary Sciences, 43:299–331.

Edmond, J. 1992. Himalayan tectonics, weathering processes, and the strontium isotope record in marine limestones. Science, 258:1594–1597.

Ellis, A., T. M. Johnson, and T. D. Bullen. 2002. Chromium isotopes and the fate of hexavalent chromium in the environment. Science, 295:2060–2062.

Ellis, A., T. M. Johnson, and T. D. Bullen. 2004. Using chromium stable isotope ratios to quantify Cr(VI) reduction: Lack of sorption effects: Environmental Science & Technology, 38:3604–3607.

Emerson, S. R., and S. S. Huested. 1991. Ocean anoxia and the concentrations of molybdenum and vanadium in seawater. Marine Chemistry, 34(3–4): 177–196.

Endal, A. S., and K. H. Schatten. 1982. The faint young sun-climate paradox: Continental influences. Journal of Geophysical Research: Oceans (1978–2012), 87(C9):7295–7302.

Ernst, R. E., M. T. D. Wingate, K. L. Buchan, and Z. X. Li. 2008. Global record of 1600–700 Ma large igneous provinces (LIPs): Implications for the reconstruction of the proposed Nuna (Columbia) and Rodinia supercontinents. Precambrian Research, 160(1–2):159–178.

Ernst, R. E., W. Bleeker, U. Söderlund, and A. C. Kerr. 2013. Large Igneous Provinces and supercontinents: Toward completing the plate tectonic revolution. Lithos, 174:1–14.

Erwin, D. H., M. Laflamme, S. M. Tweedt, E. A. Sperling, D. Pisani, and K. J. Peterson. 2011. The Cambrian conundrum: Early divergence and later ecological success in the early history of animals. Science, 334:1091–1097.

Evans, D. A. D. 2003. A fundamental Precambrian–Phanerozoic shift in earth's glacial style? Tectonophysics, 375(1–4):353–385.

Evans, D. A., N. J. Beukes, and J. L. Kirschvink. 1997. Low-latitude glaciation in the Palaeoproterozoic Era. Nature, 386:262–266.

Evans, D. A. D. 2013. Reconstructing pre-Pangean supercontinents. Geological Society of America Bulletin, 125(11–12):1735–1751.

Evans, D. A. D., and R. N. Mitchell. 2011. Assembly and breakup of the core of Paleoproterozoic–Mesoproterozoic supercontinent Nuna. Geology, 39:443–446.

Feely, R. A., J. H. Trefry, G. T. Lebon and C. R. German. 1998. The relationship between P/Fe and V/Fe ratios in hydrothermal precipitates and dissolved phosphate in seawater. Geophysical Research Letters, 25:2253–2256.

Fendorf, S. E. 1995. Surface reactions of chromium in soils and waters. Geoderma, 67: 55–71.

Fennel, K., M. Follows, and P. G. Falkowski. 2005. The co-evolution of the nitrogen, carbon and oxygen cycles in the Proterozoic ocean. American Journal of Science, 305:526–545.

Fischer, G., and G. Karakas. 2009. Sinking rates and ballast composition of particles in the Atlantic Ocean: Implications for the organic carbon fluxes to the deep ocean. Biogeosciences, 6:85–102.

Fischer, G., G. Karakas, M. Blaas, V. Ratmeyer, N. Nowald, R. Schlitzer, P. Helmke, R. Davenport, B. Donner, S. Neuer, and G. Wefer. 2009. Mineral ballast and particle settling rates in the coastal upwelling system off NW Africa and the South Atlantic. International Journal of Earth Sciences, 98:281–298.

Fralick, P., and J.E. Carter. 2011. Neoarchean deep marine paleotemperature: Evidence from turbidite successions. Precambrian Research, 191 (1–2), 78–84.

Frei, R., C. Gaucher, S.W. Poulton and D.E. Canfield. 2009. Fluctuations in Precambrian atmospheric oxygenation recorded by chromium isotopes. Nature, 461: 250–225.

French, K. L., C. Hallmann, J. M. Hope, P. L. Schoon, J. A. Zumberge, Y. Hoshino, C. A. Peters, S. C. George, G. D. Love, J. J. Brocks, R. Buick, and R. E. Summons. 2015. Reappraisal of hydrocarbon biomarkers in Archean rocks. Proceedings of the

National Academy of Sciences, 112:5915–5920.
Geboy, N. J., A. J. Kaufman, R. J. Walker, A. Misi, T. F. De Oliviera, K. E. Miller, K. Azmy, B. Kendall, and S. W. Poulton. 2013. Re–Os age constraints and new observations of Proterozoic glacial deposits in the Vazante Group, Brazil. Precambrian Research, 238:199–213.
Goddéris, Y., Y. Donnadieu, A. Nédélec, B. Dupré, C. Dessert, A. Grard, G. Ramstein, and L. M. François. 2003. The Sturtian 'Snowball' glaciation: Fire and ice. Earth and Planetary Science Letters, 211(1–2):1–12.
Golonka, J., and M. Krobicki. 2012. Upwelling regime in the Carpathian Tethys: a Jurassic–Cretaceous palaeogeographic and paleoclimatic perspective. Geological Quarterly, 45:15–32.
Gomes, M. L., and M. T. Hurtgen. 2015. Sulfur isotope fractionation in modern euxinic systems: Implications for paleoenvironmental reconstructions of paired sulfate-sulfide isotope records. Geochimica et Cosmochimica Acta, 157:39–55.
Gough, D. O. 1981. Solar interior structure and luminosity variations. P. 21–34. *In* V. Domingo (ed.), Physics of Solar Variations. Springer Netherlands.
Graham, A. M. and E. J. Bouwer. 2010. Rates of hexavalent chromium reduction in anoxic estuarine sediments: pH effects and the role of acid volatile sulfides. Environmental Science and Technology, 44: 136–142.
Grantham, P. J., and L. L. Wakefield. 1988. Variations in the sterane carbon number distributions of marine source rock derived crude oils through geological time. Organic Geochemistry, 12:61–73.
Grey, K., and C. R. Calver. 2007. Correlating the Ediacaran of Australia, p. 286:115–135. *In* P. Vickers-Rich and P. Komarower (eds.), Rise and Fall of the Ediacaran Biota, Geological Society of London Special Publication, 286.
Grey, K., and I. R. Williams. 1990. Problematic bedding-plane markings from the middle Proterozoic Manganese Subgroup, Bangemall Basin, Western Australia. Precambrian Research, 46:307–327.
Grosjean, E., G. D. Love, C. Stalvies, D. A. Fike, and R. E. Summons. 2009. Origin of petroleum in the Neoproterozoic–Cambrian South Oman Salt Basin. Organic Geochemistry, 40:87–110.
Gurnis, M. 1988. Large-scale mantle convection and the aggregation and dispersal of supercontinents: Nature, 332:695–699.
Halverson, G. P., F. Ö. Dudás, A. C. Maloof, and S. A. Bowring. 2007. Evolution of the $^{87}Sr/^{86}Sr$ composition of Neoproterozoic seawater. Palaeogeography, Palaeoclimatology, Palaeoecology, 256(3–4):103–129.
Halverson, G. P., B. P. Wade, M. T. Hurtgen, and K. M. Barovich. 2010. Neoproterozoic chemostratigraphy. Precambrian Research, 182:337–350.
Hastings, D. W., S. R. Emerson and A. C. Mix. 1996. Vanadium in foraminiferal calcite as a tracer for changes in the areal extent of reducing sediments. Paleoceanography, 11:665–678.
He, Y. H., G. C. Zhao, M. Sun, and X. P. Xia. 2009. SHRIMP and LA-ICP-MS zircon geochronology of the Xiong'er volcanic rocks: Implications for the Paleo-Mesoproterozoic evolution of the southern margin of the North China Craton. Precambrian Research, 168(3–4):213–222.
Hedges, S. B., J. E. Blair, M. L. Venturi, And J. L. Shoe. 2004. A molecular timescale of eukaryote evolution and the rise of complex multicellular life. BMC Evolutionary Biology, 4:2.
Hoffman, P. F., A. J. Kaufman, G. P. Halverson, and D. P. Schrag. 1998. A Neoproterozoic Snowball Earth. Science, 281:1342–1346.
Hoffman, P. F., and D. P. Schrag. 2002. The Snowball Earth hypothesis: testing the limits of global change. Terra Nova, 14:129–155.
Holland, H. D. 1973. The oceans: A possible source of iron in iron-formations: Economic Geology, 68:1169–1172.
Hood, A. V. S., and M. W. Wallace. 2015. Extreme ocean anoxia during the Late Cryogenian recorded in reefal carbonates of Southern Australia. Precambrian Research, 261:96–111.
Horton, F. 2015. Did phosphorus derived from the weathering of large igneous provinces fertilize the Neoproterozoic ocean? Geochemistry, Geophysics, Geosystems, 16:1525–2027.
Howarth, R. W. 1988. Nutrient limitation of net primary production in marine ecosystems. Annual Review of Ecology and Systematics, 19:89–110.
Husson, J. M., A. C. Maloof, and B. Schoene. 2012. A syn-depositional age for Earth's deepest ^{13}C excursion required by isotope conglomerate tests: Terra Nova, 24:318–325.
Husson, J. M., A. C. Maloof, B. Schoene, C.Y. Chen, and J. A. Higgins. 2015. Stratigraphic expression of Earth's deepest $d^{13}C$ excursion in the Wonoka Formation of South Australia. American Journal of Science, 315:1–45.
Iversen, M. H., and L. K. Poulsen. 2007. Coprorhexy, coprophagy, and coprochaly in the copepods *Calanus helgolandicus*, *Pseudocalanus elongatus*, and *Oithona similis*. Marine Ecology Progress, Series, 350:79–89.
Javaux, E. J. 2007. The early eukaryotic fossil record. Eukaryotic Membranes and Cytoskeleton: Origins and Evolution, 607:1–19.
Javaux, E. J., A. H. Knoll, and M. R. Walter. 2001. Morphological and ecological complexity in early eukaryotic ecosystems. Nature, 412:66–69.
Javaux, E. J., A. H. Knoll, and M. R. Walter. 2004.

TEM evidence for eukaryotic diversity in mid-Proterozoic oceans. Geobiology, 2:121–132.

Javaux, E. J., C. P. Marshall, and A. Bekker. 2010. Organic-walled microfossils in 3.2-billion-year-old shallow-marine siliciclastic deposits. Nature, 463:934–8.

Jensen, S. 2003. The Proterozoic and earliest Cambrian trace fossil record; Patterns, problems and perspectives. Integrative and Comparative Biology, 43:219–228.

Jensen, S., M. L. Droser, and J. G. Gehling. 2006. A critical look at the Ediacaran trace fossil record. P. 115–157. *In* S. Xiao, and A. J. Kaufman (eds.), Neoproterozoic Geobiology and Paleobiology, Springer.

Johnson, T. M., and T. D. Bullen. 2004. Mass-dependent fractionation of selenium and chromium isotopes in low-temperature environments. P. 289–317. *In* C. M. Johnson, B. L. Beard, and F. Albarede (eds.), Geochemistry of Non-Traditional Stable Isotopes. Mineralogical Society of America, Chantilly, VA.

Johnston, D. T. 2011. Multiple sulfur isotopes and the evolution of Earth's surface sulfur cycle. Earth-Science Reviews, 106(1–2):161–183.

Johnston, D. T., J. Farquhar, and D. E. Canfield. 2007. Sulfur isotope insights into microbial sulfate reduction: When microbes meet models. Geochimica et Cosmochimica Acta, 71:3929–3947.

Johnston, D. T., S. W. Poulton, C. Dehler, S. Porter, J. Husson, D. E. Canfield, and A. H. Knoll. 2010. An emerging picture of Neoproterozoic ocean chemistry: Insights from the Chuar Group, Grand Canyon, USA: Earth and Planetary Science Letters, 290(1–2):64–73.

Jones, C., S. Nomosatryo, S. A. Crowe, C. J. Bjerrum, and D. E. Canfield. 2015. Iron oxides, divalent cations, silica, and the early Earth phosphorus crisis. Geology, 43:135–138.

Kah, L. C., D. C. Crawford, J. K. Bartley, V. I. Kozlov, N. D. Sergeeva, and V. N. Puchkov. 2007. C-and Sr-isotope chemostratigraphy as a tool for verifying age of Riphean deposits in the Kama-Belaya aulacogen, the east European platform. Stratigraphy and Geological Correlation, 15:12–29.

Kah, L. C., A. G. Sherman, G. M. Narbonne, A. H. Knoll, and A. J. Kaufman. 1999. $\delta^{13}C$ stratigraphy of the Proterozoic Bylot Supergroup, Baffin Island, Canada: Implications for regional lithostratigraphic correlations. Canadian Journal of Earth Sciences, 36:313–332.

Karhu, J.A., and S. Epstein. 1986. The implication of the oxygen isotope records in coexisting cherts and phosphates. Geochimica et Cosmochimica Acta, 50:1745–1756.

Karhu, J. A., and H. D. Holland. 1996. Carbon isotopes and the rise of atmospheric oxygen. Geology, 24:867–870.

Kasting, J. F. 2005. Methane and climate during the Precambrian era. Precambrian Research, 137(3–4):119–129.

Kasting, J. F., K. J. Zahnle, J. P. Pinto, and A. T. Young. 1989. Sulfur, ultraviolet radiation, and the early evolution of life. Origins of Life and Evolution of the Biosphere, 19:95–108.

Katsev, S and S.A. Crowe, 2105, Organic carbon burial efficiencies in sediments: The power law of mineralization revisited. Geology, 43:607–610.

Kelemen, P. B., and C. E. Manning. 2015. Reevaluating carbon fluxes in subduction zones, what goes down, mostly comes up. Proceedings of the National Academy of Sciences, doi: 10.1073/pnas.1507889112.

Kendall, B., R. A. Creaser, G. W. Gordon, and A. D. Anbar. 2009. Re–Os and Mo isotope systematics of black shales from the Middle Proterozoic Velkerri and Wollogorang Formations, McArthur Basin, northern Australia. Geochimica et Cosmochimica Acta, 73:2534–2558.

Kirschvink, J. 1992. Late Proterozoic low-latitude global glaciation: the Snowball Earth, p. 51–52. *In* J. W. Schopf and C. Klein (eds.), The Proterozoic Biosphere: A Multidisciplinary Study. Cambridge University Press.

Kirschvink, J., T. Raub, And W. Fischer. 2012. Archean "whiffs of oxygen" go poof! p. 1943. 22nd Goldschmidt Conference Abstracts, Montréal, Canada.

Klaas, C., and D. E. Archer. 2002. Association of sinking organic matter with various types of mineral ballast in the deep sea: Implications for the rain ratio. Global Biogeochemical Cycles, 16(4):63-1–63-14.

Knauth, L. P., and M. J. Kennedy. 2009. The late Precambrian greening of the Earth. Nature, 460:728–732.

Knoll, A. H. 2014. Paleobiological perspectives on early eukaryotic evolution. Cold Spring Harbor Perspectives in Biology, 6:aO16121. doi: 10.1101/cshperspect.a01612.

Knoll, A. H., E. J. Javaux, D. Hewitt, and P. Cohen. 2006. Eukaryotic organisms in Proterozoic oceans. Philosophical Transactions of the Royal Society B-Biological Sciences, 361:1023–1038.

Kodner, R. B., R. E. Summons, A. Pearson, N. King, and A. H. Knoll. 2008. Sterols in a unicellular relative of the metazoans. Proceedings of the National Academy of Sciences, 105:9897–9902.

Konhauser, K. O., S. V. Lalonde, L. Amskold, and H. D. Holland. 2007. Was there really an Archean phosphate crisis? Science, 315:1234–1234.

Kuipers, G., F. F. Beunk, and F. M. Van Der Wateren. 2013. Periglacial evidence for a 1.91–1.89 Ga old glacial period at low latitude, Central Sweden.

Geology Today, 29:218–221.
Kunzmann, M., G. P. Halverson, P. A. Sossi, T. D. Raub, J. L. Payne, and J. Kirby. 2013. Zn isotope evidence for immediate resumption of primary productivity after snowball Earth. Geology, 41:27–30.
Kuypers, M. M. M., A. O. Sliekers, G. Lavik, M. Schmid, B. B. Jorgensen, J. G. Kuenen, J. S. S. Damste, M. Strous, and M. S. M. Jetten. 2003. Anaerobic ammonium oxidation by anammox bacteria in the Black Sea. Nature. 422:608–611.
Lamb, D. M., S. M. Awramik, D. J. Chapman, and S. Zhu. 2009. Evidence for eukaryotic diversification in the ~1800 million-year-old Changzhougou Formation, North China. Precambrian Research, 173(1–4):93–104.
Lane, N., and W. Martin. 2010. The energetics of genome complexity. Nature, 467:929–934.
Large, R. R., J. A. Halpin, L. V. Danyushevsky, V. V. Maslennikov, S. W. Bull, J. A. Long, D. D. Gregory, E. Lounejeva, T. W. Lyons, P. J. Sack, P. J. Mcgoldrick, and C. R. Calver. 2014. Trace element content of sedimentary pyrite as a new proxy for deep-time ocean–atmosphere evolution. Earth and Planetary Science Letters, 389:209–220.
Leavitt, W. D., I. Halevy, A. S. Bradley, and D. T. Johnston. 2013. Influence of sulfate reduction rates on the Phanerozoic sulfur isotope record: Proceedings of the National Academy of Sciences, 110:11244–11249.
Lee, C.-T. A., B. Shen, B. S. Slotnick, K. Liao, G. R. Dickens, Y. Yokoyama, A. Lenardic, R. Dasgupta, M. Jellinek, J. S. Lackey, T. Schneider, and M. M. Tice. 2013. Continental arc–island arc fluctuations, growth of crustal carbonates, and long-term climate change. Geosphere, 9:21–36.
Lee, C.-T. A., S. Thurner, S. Paterson, and W. Cao. 2015. The rise and fall of continental arcs: Interplays between magmatism, uplift, weathering, and climate. Earth and Planetary Science Letters, 425:105–119.
Li, C., P. Peng, G. Y. Sheng, J. M. Fu, and Y. Z. Yan. 2003. A molecular and isotopic geochemical study of Meso- to Neoproterozoic (1.73–0.85 Ga) sediments from the Jixian section, Yanshan Basin, North China. Precambrian Research, 125(3–4): 337–356.
Li, Z.-X., D. A. D. Evans, and G. P. Halverson. 2013. Neoproterozoic glaciations in a revised global palaeogeography from the breakup of Rodinia to the assembly of Gondwanaland. Sedimentary Geology, 294:219–232.
Li, Z.X., and Zhong, S. 2009. Supercontinent–superplume coupling, true polar wander and plume mobility: Plate dominance in whole-mantle tectonics: Physics of the Earth and Planetary Interiors, 176, 143–156.
Liu, C., Z. Wang, T. D. Raub, F. A. Macdonald, and D. A. Evans. 2014. Neoproterozoic cap-dolostone deposition in stratified glacial meltwater plume. Earth and Planetary Science Letters, 404:22–32.
Logan, G. A., J. M. Hayes, G. B. Hieshima, and R. E. Summons. 1995. Terminal Proterozoic reorganization of biogeochemical cycles. Nature, 376:53–56.
Love, G. D., E. Grosjean, C. Stalvies, D. A. Fike, J. P. Grotzinger, A. S. Bradley, A. E. Kelly, M. Bhatia, W. Meredith, C. E. Snape, S. A. Bowring, D. J. Condon, and R. E. Summons. 2009. Fossil steroids record the appearance of Demospongiae during the Cryogenian period. Nature, 457:718–721.
Love, G. D., C. E. Snape, A. D. Carr, and R. C. Houghton. 1995. Release of covalently-bound alkane biomarkers in high yields from kerogen via catalytic hydropyrolysis. Organic Geochemistry, 23(10):981–986.
Love, G. D., and R. E. Summons. In press. The molecular record of Cryogenian sponges—a response to Antcliffe (2013). Palaeontology.
Lyons, T. W., C. T. Reinhard, G. D. Love, And S. Xiao. 2012. Geobiology of the Proterozoic Eon. *In* A. H. Knoll, D. E. Canfield, and K. O. Konhauser (eds.), Fundamentals of Geobiology. John Wiley & Sons, Chichester. doi: 10.1002/9781118280874.ch20.
Lyons, T. W., C. T. Reinhard, and N. J. Planavsky. 2014. The rise of oxygen in Earth's early ocean and atmosphere. Nature, 506:307–315.
Lyons, T. W., and S. Severmann. 2006. A critical look at iron paleoredox proxies: New insights from modern euxinic marine basins. Geochimica et Cosmochimica Acta, 70:5698–5722.
Marin-Carbonne, J., F. Robert, and M. Chaussidon. 2014. The silicon and oxygen isotope-compositions of Precambrian cherts: A record of oceanic paleo-temperatures? Precambrian Research, 247:223–234.
Marriott, C. S., G. M. Henderson, R. Crompton, M. Staubwasser, and S. Shaw. 2004. Effect of mineralogy, salinity, and temperature on Li/Ca and Li isotope composition of calcium carbonate. Chemical Geology, 212(1–2):5–15.
Martin, W., and M. Muller. 1998. The hydrogen hypothesis for the first eukaryote. Nature ,392:37–41.
McArthur, J., R. Howarth, and G. Shields. 2012. Strontium isotope stratigraphy, p. 127–144. *In* F. M. Gradstein, J. G. Ogg M. D. Schmitz, and G. M. Ogg (eds.),The Geologic Time Scale. Elsevier,
McCaffrey, M. A., J. M. Moldowan, P. A. Lipton, R. E. Summons, K. E. Peters, A. Jeganathan, and D. S. Watt. 1994. Paleoenvironmental implications of novel C-30 steranes in Precambrian to Cenozoic age petroleum and bitumen. Geochimica et Cosmochimica Acta, 58:529–532.
McKenzie, N. R., N. C. Hughes, B. C. Gill, and P. M. Myrow. 2014. Plate tectonic influences on

Neoproterozoic–early Paleozoic climate and animal evolution. Geology, 42:127–130.

McKirdy, D. M., L. J. Webster, K. R. Arouri, K. Grey, and V. A. Gostin. 2006. Contrasting sterane signatures in Neoproterozoic marine rocks of Australia before and after the Acraman asteroid impact. Organic Geochemistry, 37:189–207.

Meert, J. G. 2012. What's in a name? The Columbia (Paleopangaea/Nuna) supercontinent: Gondwana Research, 21:987–993.

Mills, D. B., L. M. Ward, C. Jones, B. Sweeten, M. Forth, A. H. Treusch, and D. E. Canfield. 2014. Oxygen requirements of the earliest animals. Proceedings of the National Academy of Sciences, 111:4168–4172.

Mitchell, R. L., and Sheldon, N. D. 2010. The ~1100 Ma Sturgeon Falls paleosol revisited: Implications for Mesoproterozoic weathering environments and atmospheric CO2 levels. Precambrian Research, 183:738–748.

Moldowan, J. M., F. J. Fago, C. Y. Lee, S. R. Jacobson, D. S. Watt, N. E. Slougui, A. Jeganathan, and D. C. Young. 1990. Sedimentary 24-n-propylcholestanes, molecular fossils diagnostic of marine algae. Science, 247:309–312.

Moreira, D., and P. Lopez-Garcia. 1998. Symbiosis between methanogenic archaea and δ-proteobacteria as the origin of eukaryotes: The syntrophic hypothesis. Journal of Molecular Evolution, 47:517–530.

Moroz, L. L., K. M. Kocot, M. R. Citarella, S. Dosung, T. P. Norekian, I. S. Povolotskaya, A. P. Grigorenko, C. Dailey, E. Berezikov, K. M. Buckley, A. Ptitsyn, D. Reshetov, K. Mukherjee, T. P. Moroz, Y. Bobkova, F. H. Yu, V. V. Kapitonov, J. Jurka, Y. V. Bobkov, J. J. Swore, D. O. Girardo, A. Fodor, F. Gusev, R. Sanford, R. Bruders, E. Kittler, C. E. Mills, J. P. Rast, R. Derelle, V. V. Solovyev, F. A. Kondrashov, B. J. Swalla, J. V. Sweedler, E. I. Rogaev, K. M. Halanych, and A. B. Kohn. 2014. The ctenophore genome and the evolutionary origins of neural systems. Nature, 510:109–114.

Morse, J. W., J. J. Zullig, L. D. Bernstein, F. J. Millero, P. J. Milne, A. Mucci, and G. R. Choppin. 1985. Chemistry of calcium carbonate-rich shallow water sediments in the Bahamas. American Journal of Science, 285:147–185.

Müller, R. D., M. Sdrolias, C. Gaina, and W. R. Roest. 2008. Age, spreading rates, and spreading asymmetry of the world's ocean crust. Geochemistry, Geophysics, Geosystems, 9(4)1–19.

Nance, R. D., J. B. Murphy, and M. Santosh. 2014. The supercontinent cycle: A retrospective essay. Gondwana Research, 25:4–29.

Neuweiler, F., E. C. Turner, and D. J. Burdige. 2009. Early Neoproterozoic origin of the metazoan clade recorded in carbonate rock texture. Geology, 37:475–478.

Noordmann, J., S. Weyer, C. Montoya-Pino, O. Dellwig, N. Neubert, S. Eckert, M. Paetzel, and M. E. Bottcher. 2015. Uranium and molybdenum isotope systematics in modern euxinic basins: Case studies from the central Baltic Sea and the Kyllaren Fjord (Norway). Chemical Geology, 396:182–195.

Nursall, J. 1959. Oxygen as a prerequisite to the origin of the Metazoa. Nature, 183:1170–1172.

Ohnemueller, F., A. R. Prave, A. E. Fallick, and S. A. Kasemann. 2014. Ocean acidification in the aftermath of the Marinoan glaciation. Geology, 42:1103–1106.

Olson, S. L., L. R. Kump, and J. F. Kasting. 2013. Quantifying the areal extent and dissolved oxygen concentrations of Archean oxygen oases. Chemical Geology, 362:35–43.

Palike, H., M. W. Lyle, H. Nishi, I. Raffi, A. Ridgwell, K. Gamage, A. Klaus, G. Acton, L. Anderson, J. Backman, J. Baldauf, C. Beltran, S. M. Bohaty, Bownpaul, W. Busch, J. E. T. Channell, C. O. J. Chun, M. Delaney, P. Dewangan, T. Dunkley Jones, K. M. Edgar, H. Evans, P. Fitch, G. L. Foster, N. Gussone, H. Hasegawa, E. C. Hathorne, H. Hayashi, J. O. Herrle, A. Holbourn, S. Hovan, K. Hyeong, K. Iijima, T. Ito, S.-I. Kamikuri, K. Kimoto, J. Kuroda, L. Leon-Rodriguez, A. Malinverno, T. C. Moore Jr, B. H. Murphy, D. P. Murphy, H. Nakamura, K. Ogane, C. Ohneiser, C. Richter, R. Robinson, E. J. Rohling, O. Romero, K. Sawada, H. Scher, L. Schneider, A. Sluijs, H. Takata, J. Tian, A. Tsujimoto, B. S. Wade, T. Westerhold, R. Wilkens, T. Williams, P. A. Wilson, Y. Yamamoto, S. Yamamoto, T. Yamazaki, and R. E. Zeebe. 2012. A Cenozoic record of the equatorial Pacific carbonate compensation depth. Nature, 488:609–614.

Palmer, M. R., and J. M. Edmond. 1989. The strontium isotope budget of the modern ocean. Earth and Planetary Science Letters, 92:11–26.

Pan, Y.M. and M.R. Stauffer. 2000. Cerium anomaly and Th/U fractionation in the 1.85 Ga Flin Flon Paleosol: Clues from REE- and U-rich accessory minerals and implications for paleoatmospheric reconstruction. American Mineralogy, 85:898–911.

Pang, K., Q. Tang, J. D. Schiffbauer, J. Yao, X. Yuan, B. Wan, L. Chen, Z. Ou, and S. Xiao. 2013. The nature and origin of nucleus-like intracellular inclusions in Paleoproterozoic eukaryote microfossils. Geobiology, 11:499–510.

Pang, K., Q. Tang, X.-L. Yuan, B. Wan, and S. Xiao. 2015. A biomechanical analysis of the early eukaryotic fossil *Valeria* and new occurrence of organic-walled microfossils from the Paleo-Mesoproterozoic Ruyang Group. Palaeoworld,

doi:10.1016/j.palwor.2015.04.002.

Partin, C. A., A. Bekker, N. J. Planavsky, C. T. Scott, B. C. Gill, C. Li, V. Podkovyrov, A. Maslov, K. O. Konhauser, S. V. Lalonde, G. D. Love, S. W. Poulton, and T. W. Lyons. 2013a. Large-scale fluctuations in Precambrian atmospheric and oceanic oxygen levels from the record of U in shales. Earth and Planetary Science Letters, 369:284–293.

Partin, C. A., S. V. Lalonde, N. J. Planavsky, A. Bekker, O. J. Rouxel, T. W. Lyons, and K. O. Konhauser. 2013b. Uranium in iron formations and the rise of atmospheric oxygen. Chemical Geology, 362:82–90.

Pavlov, A. A., M. T. Hurtgen, J. F. Kasting, And M. A. Arthur. 2003. Methane-rich Proterozoic atmosphere? Geology, 31:87–90.

Pavlov, A. A., J. F. Kasting, L. L. Brown, K. A. Rages, and R. Freedman. 2000. Greenhouse warming by CH4 in the atmosphere of early Earth. Journal of Geophysical Research: Planets (1991–2012), 105(E5):11981–11990.

Pawlowska, M. M., N. J. Butterfield, and J. J. Brocks. 2013. Lipid taphonomy in the Proterozoic and the effect of microbial mats on biomarker preservation. Geology, 41:103–106.

Pecoits, E., K. O. Konhauser, N. R. Aubet, L. M. Heaman, G. Veroslavsky, R. A. Stern, and M. K. Gingras. 2012. Bilaterian burrows and grazing behavior at > 585 million years ago. Science, 336(6089):1693–1696.

Pehrsson, S. J., B. M. Eglington, D. A. D. Evans, D. Huston, and S. M. Reddy. 2015. Metallogeny and its link to orogenic style during the Nuna supercontinent cycle. The Geological Society of London Special Publications, 424. doi:10.1144/SP424.5.

Peng, Y. B., H. M. Bao, and X. L. Yuan. 2009. New morphological observations for Paleoproterozoic acritarchs from the Chuanlinggou Formation, North China. Precambrian Research, 168(3–4): 223–232.

Petit, J. R., J. Jouzel, D. Raynaud, N. I. Barkov, J. M. Barnola, I. Basile, M. Bender, J. Chappellaz, M. Davis, G. Delaygue, M. Delmotte, V. M. Kotlyakov, M. Legrand, V. Y. Lipenkov, C. Lorius, L. Pepin, C. Ritz, E. Saltzman, and M. Stievenard. 1999. Climate and atmospheric history of the past 420,000 years from the Vostok ice core, Antarctica. Nature, 399:429–436.

Pisarevsky, S. A., S.-Å. Elming, L. J. Pesonen, and Z.-X. Li. 2014. Mesoproterozoic paleogeography: Supercontinent and beyond. Precambrian Research, 244:207–225.

Planavsky, N. 2009. Early Neoproterozoic origin of the metazoan clade recorded in carbonate rock texture: COMMENT. Geology, 37(9):E195–E195.

Planavsky, N. J., A. Bekker, A. Hofmann, J. D. Owens, and T. W. Lyons. 2012. Sulfur record of rising and falling marine oxygen and sulfate levels during the Lomagundi event: Proceedings of the National Academy of Sciences, 109:18300–18305.

Planavsky, N. J., P. McGoldrick, C. T. Scott, C. Li, C. T. Reinhard, A. E. Kelly, X. L. Chu, A. Bekker, G. D. Love, and T. W. Lyons. 2011. Widespread iron-rich conditions in the mid-Proterozoic ocean. Nature, 477:448–U95.

Planavsky, N. J., C. T. Reinhard, X. Wang, D. Thomson, P. Mcgoldrick, R. H. Rainbird, T. Johnson, W. W. Fischer, and T. W. Lyons. 2014. Low Mid-Proterozoic atmospheric oxygen levels and the delayed rise of animals. Science, 346:635–638.

Planavsky, N., O. Rouxel, A. Bekker, S. Lalonde, K. O. Konhauser, C. T. Reinhard, and T. W. Lyons. 2010. The evolution of the marine phosphate reservoir. Nature, 467:1088–1090.

Ploug, H., M. H. Iversen, and G. Fischer. 2008. Ballast, sinking velocity, and apparent diffusivity within marine snow and zooplankton fecal pellets: Implications for substrate turnover by attached bacteria. Limnology and Oceanography, 53:1878–1886.

Pogge Von Strandmann, P. A. E., and G. M. Henderson. 2014. The Li isotope response to mountain uplift. Geology, doi: 10.1130/G36162.1

Porter, S. 2011. The rise of predators. Geology, 39:607–608.

Porter, S. M., R. Meisterfeld, and A. H. Knoll. 2003. Vase-shaped microfossils from the Neoproterozoic Chuar Group, Grand Canyon: A classification guided by modern testate amoebae. Journal of Paleontology, 77:409–429.

Poulton, S. W., and D. E. Canfield. 2005. Development of a sequential extraction procedure for iron: implications for iron partitioning in continentally derived particulates. Chemical Geology, 214(3–4): 209–221.

Poulton, S. W., and D. E. Canfield. 2011. Ferruginous conditions: A dominant feature of the ocean through Earth's history. Elements, 7:107–112.

Poulton, S. W., P. W. Fralick, and D. E. Canfield. 2004. The transition to a sulphidic ocean similar to 1.84 billion years ago. Nature, 431(7005):173–177.

Pratt, L. M., R. E. Summons, and G. B. Hieshima. 1991. Sterane and triterpane biomarkers in the Precambrian Nonesuch Formation, North American Midcontinent Rift. Geochimica et Cosmochimica Acta, 55(3):911–916.

Pufahl, P. K., and E. E. Hiatt. 2012. Oxygenation of the Earth's atmosphere–ocean system: A review of physical and chemical sedimentologic responses. Marine and Petroleum Geology, 32:1–20.

Rauch, J. N., and J. M. Pacyna. 2009. Earth's global Ag, Al, Cr, Cu, Fe, Ni, Pb, and Zn cycles. Global Biogeochemical Cycles, 23:GB2001, doi:

10.1029/2008GB003376.

Redfield, A. C. 1934. On the proportions of organic derivations in sea water and their relation to the composition of plankton, p. 177–192. *In* R. J. Daniel (ed.), James Johnstone Memorial Volume, University Press of Liverpool, Liverpool, UK.

Reinhard, C. T., S. V. Lalonde, and T. W. Lyons. 2013a. Oxidative sulfide dissolution on the early Earth. Chemical Geology, 362:44–55.

Reinhard, C. T., N. J. Planavsky, L. J. Robbins, C. A. Partin, B. C. Gill, S. V. Lalonde, A. Bekker, K. O. Konhauser, and T. W. Lyons. 2013b. Proterozoic ocean redox and biogeochemical stasis: Proceedings of the National Academy of Sciences, 110:5357–5362.

Richard, F. C. and A. C. M. Bourg. 1991. Aqueous geochemistry of chromium—a review. Water Research 25, 807–816.

Ridgwell, A., and R. E. Zeebe. 2005. The role of the global carbonate cycle in the regulation and evolution of the Earth system. Earth and Planetary Science Letters, 234(3–4):299–315.

Robert, F., and M. Chaussidon. 2006. A palaeotemperature curve for the Precambrian oceans based on silicon isotopes in cherts. Nature, 443: 969–972.

Rodrigues, J. B., M. M. Pimentel, B. Buhn, M. Matteini, M. A. Dardenne, C. J. S. Alvarenga, and R. A. Armstrong. 2012. Provenance of the Vazante Group: New U–Pb, Sm–Nd, Lu–Hf isotopic data and implications for the tectonic evolution of the Neoproterozoic Brasília Belt. Gondwana Research, 21(2–3):439–450.

Rooney, A. D., J. V. Strauss, A. D. Brandon, and F. A. Macdonald. 2015. A Cryogenian chronology: Two long-lasting synchronous Neoproterozoic glaciations. Geology, 43:459–462.

Rowley, D. B. 2002. Rate of plate creation and destruction: 180 Ma to present. Geological Society of America Bulletin, 114(8):927–933.

Runnegar, B. 1991. Precambrian oxygen levels estimated from the biochemistry and physiology of early eukaryotes. Palaeogeography, Palaeoclimatology, Palaeoecology, 97(1–2):97–111.

Rye, R. and H. D. Holland. 1998. Paleosols and the evolution of atmospheric oxygen: a critical review. American Journal of Science, 298: 621–672.

Sahoo, S. K., N. J. Planavsky, B. Kendall, X. Q. Wang, X. Y. Shi, C. Scott, A. D. Anbar, T. W. Lyons, and G. Q. Jiang. 2012. Ocean oxygenation in the wake of the Marinoan glaciation. Nature, 489:546–549.

Schauble, E. A., G. R. Rossman, and H. P. J. Taylor. 2004. Theoretical estimates of equilibrium chromium-isotope fractionations. Chemical Geology, 205:99–114.

Schoenberg, R., S. Zink, M. Staubwasser, and F. Von Blanckenburg. 2008. The stable Cr isotope inventory of solid Earth reservoirs determined by double spike MC-ICP-MS. Chemical Geology, 249(3–4):294–306.

Schrag, D. P., R. A. Berner, P. F. Hoffman, and G. P. Halverson. 2002. On the initiation of a Snowball Earth. Geochemistry Geophysics Geosystems, 3: doi: 10.1029/2001gc000219.

Schrag, D. P., J. A. Higgins, F. A. Macdonald, and D. T. Johnston. 2013. Authigenic carbonate and the history of the global carbon cycle. Science, 339:540–543.

Schulz, H. N., T. Brinkhoff, T. G. Ferdelman, M. H. Marine, A. Teske, and B. B. Jorgensen. 1999. Dense populations of a giant sulfur bacterium in Namibian shelf sediments. Science 284:493–495.

Schwark, L., and P. Empt. 2006. Sterane biomarkers as indicators of Palaeozoic algal evolution and extinction events. Palaeogeography Palaeoclimatology Palaeoecology, 240(1–2):225–236.

Scott, C., T. W. Lyons, A. Bekker, Y. Shen, S. Poulton, X. Chu, and A. Anbar. 2008. Tracing the stepwise oxygenation of the Proterozoic biosphere. Nature, 452:456–459.

Scott, C., B. A. Wing, A. Bekker, N. J. Planavsky, P. Medvedev, S. M. Bates, M. Yun, and T. W. Lyons. 2014. Pyrite multiple-sulfur isotope evidence for rapid expansion and contraction of the early Paleoproterozoic seawater sulfate reservoir. Earth and Planetary Science Letters, 389:95–104.

Sheldon, N. D. 2013, Causes and consequences of low atmospheric pCO(2) in the late Mesoproterozoic. Chemical Geology, 362: 224–231.

Singh, H. B., and J. F. Kasting. 1988. Chlorine-hydrocarbon photochemistry in the marine troposphere and lower stratosphere. Origins of Life and Evolution of the Biosphere, 7:261–285.

Sim, M. S., T. Bosak, and S. Ono. 2011. Large sulfur isotope fractionation does not require disproportionation. Science, 333:74–77.

Spang, A., J. H. Saw, S. L. Jorgensen, K. Zaremba-Niedzwiedzka, J. Martijn, A. E. Lind, R. Van Eijk, C. Schleper, L. Guy, and T. J. G. Ettema. 2015. Complex Archaea that bridge the gap between prokaryotes and eukaryotes. Nature, 521:173–179.

Sperling, E. A., G. P. Halverson, A. H. Knoll, F. A. Macdonald, and D. T. Johnston. 2013. A basin redox transect at the dawn of animal life. Earth and Planetary Science Letters, 371–372:143–155.

Stanley, G. D. Jr., and W. Stürmer. 1983. The first fossil ctenophore from the lower Devonian of West Germany. Nature, 303: 518–520.

Strother, P. K., L. Battison, M. D. Brasier, and C. H. Wellman. 2011. Earth's earliest non-marine eukaryotes. Nature, 473:505–509.

Su, W., H. Li, L. Xu, S. Jia, J. Geng, H. Zhou, Z. Wang, and H. Pu. 2012. Luoyu and Ruyang Group at the south margin of the North China Craton

(NCC) should belong in the Mesoproterozoic Changchengian System: Direct constraints from the LA-MC-ICPMS U-Pb age of the tuffite in the Luoyukou Formation, Ruzhou, Henan, China. Geological Survey and Research, 35:96–108.

Summons, R. E., A. S. Bradley, L. L. Jahnke, and J. R. Waldbauer. 2006. Steroids, triterpenoids and molecular oxygen. Philosophical Transactions of the Royal Society B-Biological Sciences, 361:951–968.

Summons, R. E., S. C. Brassell, G. Eglinton, E. Evans, R. J. Horodyski, N. Robinson, and D. M. Ward. 1988. Distinctive hydrocarbon biomarkers from fossiliferous sediment of the late Proterozoic Walcott Member, Chuar Group, Grand Canyon, Arizona. Geochimica et Cosmochimica Acta, 52:2625–2637.

Summons, R. E., J. Thomas, J. R. Maxwell, and C. J. Boreham. 1992. Secular and environmental constraints on the occurrence of dinosterane in sediments. Geochimica et Cosmochimica Acta, 56:2437–2444.

Summons, R. E., and M. R. Walter. 1990. Molecular fossils and microfossils of prokaryotes and protists from Proterozoic sediments. American Journal of Science, 290A:212–244.

Tarhan, L. G., M. L. Droser, and J. G. Gehling. 2015. Depositional and preservational environments of the Ediacara Member, Rawnsley Quartzite (South Australia): Assessment of paleoenvironmental proxies and the timing of 'ferruginization.' Palaeogeography, Palaeoclimatology, Palaeoecology, 434:4–13.

Thomson, D., R. H. Rainbird, and G. Dix. 2014. Architecture of a Neoproterozoic intracratonic carbonate ramp succession: Wynniatt Formation, Amundsen Basin, Arctic Canada. Sedimentary Geology, 299:119–138.

Towe, K. M. 1970. Oxygen-collagen priority and the early metazoan fossil record. Proceedings of the National Academy of Sciences 65:781–788.

Turner, J. T. 2002. Zooplankton fecal pellets, marine snow and sinking phytoplankton blooms. Aquatic Microbial Ecology 27:57–102.

Tyrrell, T. 1999. The relative influences of nitrogen and phosphorus on oceanic primary production. Nature, 400:525–531.

Ventura, G. T., F. Kenig, E. Grosjean, and R. E. Summons. 2004. Biomarker analysis of solvent extractable organic matter from the late Neoproterozoic Kwagunt Formation, Chuar Group (~800–742 Ma), Grand Canyon. Geological Society of America Abstracts with Programs, Vol. 36(5):170.

Volkman, J. K. 2003. Sterols in microorganisms. Applied Microbiology and Biotechnology, 60:495–506.

Volkman, J. K. 2005. Sterols and other triterpenoids: source specificity and evolution of biosynthetic pathways. Organic Geochemistry, 36:139–159.

Walter, M. R., R. L. Du, and R. J. Horodyski. 1990. Coiled carbonaceous megafossils from the middle Proterozoic of Jixian (Tianjin) and Montana. American Journal of Science, 290A:133–148.

Watson, B. 2008. Quiet revolution in the geochemical sciences. Elements, 4:219–220.

Whelan, N. V., K. M. Kocot, L. L. Moroz, and K. M. Halanych. 2015. Error, signal, and the placement of Ctenophora sister to all other animals. Proceedings of the National Academy of Sciences, 112:5773–5778.

Williams, G. E. 2005. Subglacial meltwater channels and glaciofluvial deposits in the Kimberley Basin, Western Australia: 1.8 Ga low-latitude glaciation coeval with continental assembly. Journal of the Geological Society, 162:111–124.

Williams, T. A., P. G. Foster, C. J. Cox, and T. M. Embley. 2013. An archaeal origin of eukaryotes supports only two primary domains of life. Nature, 504:231–236.

Williams, T. A., P. G. Foster, T. M. W. Nye, C. J. Cox, and T. M. Embley. 2012. A congruent phylogenomic signal places eukaryotes within the Archaea. Proceedings of the Royal Society B-Biological Sciences, 279:4870–4879.

Woese, C. R., O. Kandler, And M. L. Wheelis. 1990. Towards a natural system of organisms—proposal for the domains Archaea, Bacteria, and Eucarya. Proceedings of the National Academy of Sciences, 87:4576–4579.

Wolf, E. T., and O. B. Toon. 2014. Controls on the Archean climate system investigated with a global climate model. Astrobiology, 14:241–253.

Wordsworth, R., and R. Pierrehumbert. 2013. Hydrogen-nitrogen greenhouse warming in Earth's early atmosphere. Science, 339:64–67.

Yoon, H. S., J. D. Hackett, C. Ciniglia, G. Pinto, and D. Bhattacharya. 2004. A molecular timeline for the origin of photosynthetic eukaryotes. Molecular Biology and Evolution, 21:809–818.

Zbinden, E. A., H. D. Holland, C. R. Feakes and S. K. Dobos. 1988. The Sturgeon Falls Paleosol and the composition of the atmosphere 1.1 Ga Bp. Precambrian Research, 42:141–163.

Zink, S., R. Schoenberg, and M. Staubwasser. 2010. Isotopic fractionation and reaction kinetics between Cr(III) and Cr(VI) in aqueous media. Geochimica et Cosmochimica Acta, 74:5729–5745.